UCSF

UC San Francisco Previously Published Works

Title

Magnetic Resonance Imaging for Spine Emergencies.

Permalink

https://escholarship.org/uc/item/6x01r3kz

Journal

Magnetic Resonance Imaging Clinics of North America, 30(3)

Authors

Mathieu, Jeannette
Talbott, Jason

Publication Date

2022-08-01

DOI

10.1016/j.mric.2022.04.004

Peer reviewed

Magnetic Resonance Imaging for Spine Emergencies

Jeannette Mathieu, MD[1], **Jason F. Talbott, MD, PhD**[1,2]

[1]Department of Radiology and Biomedical Imaging, UCSF and Zuckerberg San Francisco General Hospital, San Francisco, CA

[2]Brain and Spinal Injury Center, Zuckerberg San Francisco General Hospital

Keywords

MRI; spinal cord; spinal cord injury; myelitis; myelopathy

Introduction

This chapter is devoted to the magnetic resonance imaging (MRI) evaluation of spine emergencies, defined as spinal pathologies that pose an immediate risk of significant morbidity or mortality to the patient if not diagnosed and treated in a timely manner. The spinal cord (SC) is exquisitely sensitive to compression and vascular compromise. Identifying signs of present or impending spinal cord compression and injury is central to the MRI search pattern for spine emergencies. In many cases, the etiology of imaging findings will be readily apparent, and the focus of spine MRI will be to describe and appropriately classify the pathology to facilitate appropriate next steps in patient management. To this end, up-to-date evidence-based imaging classification systems will be reviewed. A subset of spine emergencies is without clear etiology. In these cases, focus shifts to formulating a useful and narrow as possible differential diagnosis based on pertinent MRI findings and to assist in guiding further evaluations that may yield a definitive diagnosis, such as additional imaging, cerebral spinal fluid (CSF) studies, or biopsy. This chapter will outline a practical approach to help navigate these various scenarios and highlight key imaging features that can aid in narrowing the differential diagnosis for the most commonly encountered spine emergencies. We begin with a summary of MRI indications and MRI protocols tailored for a variety of spinal emergencies. A review of key imaging findings for the most encountered emergent spine pathologies will follow. Pathologies will be broadly grouped into traumatic and atraumatic pathologies. For traumatic injuries, a practical and algorithmic diagnostic approach based on the AO Spine injury classification system will be presented focused on subaxial spine trauma. Atraumatic spinal emergencies will be dichotomized into compressive and non-compressive subtypes. The location of external compressive disease with respect to the thecal sac is fundamental to establishing a differential diagnosis for compressive emergencies, while specific patterns

Corresponding author: Jason F. Talbott (Jason.talbott@ucsf.edu), 415-206-2942 (Phone), 415-206-4004 (Fax), Zuckerberg San Francisco General Hospital, Department of Radiology, 1001 Potrero Avenue, Room 1X57C, San Francisco, CA 94110.

of spinal cord involvement on MRI will guide the discussion of inflammatory and noninflammatory causes of non-compressive myelopathy.

ROLE OF MRI IN SPINAL EMERGENCIES

MRI is the gold standard imaging technique for many spinal emergencies. In the setting of trauma, MRI is complementary to initial first line computed tomography (CT) evaluation for a subset of patients[1,2]. The American College of Radiology (ACR) has published appropriateness criteria with recommendations for MRI as "usually appropriate" in patients with confirmed or suspected spinal cord or nerve root injury[1]. Patients with mechanically unstable spine injury for which surgical treatment is planned should also undergo spine MRI for characterization of soft tissue injuries, including unstable discoligamentous disruption, that may aid in surgical planning. Obtunded patients for whom clinical evaluation is not feasible and may have negative CT findings are also recommended for MRI by ACR criteria, although this recommendation is more controversial[3].

In cases of nontraumatic spinal emergency, MRI is usually the preferred initial imaging modality due to its excellent soft tissue contrast and ability to reliably identify compressive SC pathology[4]. The ACR has published appropriateness criteria for MRI in patients presenting with low back pain and generally limits imaging to those with red flag signs or symptoms including suspected infection, immunosuppression, chronic steroid use, suspicion for cancer, and patients with persistent or progressive symptoms following 6 weeks of conservative therapy[5]. MRI is also recommended for any patient with progressive neurologic deficits localized to the spinal cord, conus, or nerve roots/cauda equina.

MRI PROTOCOL FOR SPINAL EMERGENCIES

The ideal MRI protocol for patients with spine emergencies will vary depending on the clinical scenario. Neurologically unstable patients for whom emergent surgical intervention is needed may require an abbreviated examination tailored to address only emergent surgical questions, such as localizing the level of spinal cord compression with a rapid T2-weighted (T2W) sagittal survey of the spine and limited axial imaging at selected levels. Patients with suspected inflammatory, infectious, or neoplastic conditions may need more thorough imaging with inclusion of T1W pre- and post-contrast sequences. Fat suppression (FS) with T2W and T1W-post contrast sequences is advised whenever spinal pathology may involve extramedullary structures of the spine, such as vertebral bodies, ligaments or paraspinous tissues. When a purely non-compressive myelopathy is suspected, FS may be unnecessary and only impair signal to noise ratio or introduce unwanted artifacts for detailed spinal cord evaluation[6].

Increasingly, diffusion weighted imaging (DWI) has been incorporated into spine MRI protocols and is generally helpful whenever clinical indications would suggest a need for post-contrast imaging. This includes evaluation of the spine for infection and neoplastic pathologies. Just as in the brain, DWI may also be helpful for diagnosing patients with acute spinal cord infarcts. In the setting of traumatic spinal cord injury (SCI), many studies have evaluated diagnostic and neuroprognostic roles of DWI[7,8]. Despite intense investigation,

applications for DWI in daily clinical practice for spine trauma remain lacking and future studies are needed to validate utility of DWI beyond standard conventional sequences[9].

When spinal vascular pathology is suspected time resolved MR angiography (MRA) techniques may be useful for characterizing the nature of the vascular malformation and for potentially identifying levels of arterio-venous shunting lesions. Fat suppressed T1W sequences are particularly useful for diagnosing acute cervical arterial dissections. T2*W and susceptibility weighted imaging techniques can be useful for delineation of gray-white matter contrast and to identify intramedullary spinal cord blood products[2].

MRI for Spine Trauma

A thorough physical examination and comprehensive clinical history remain the gold standard for initial assessment of patients with acute blunt spine trauma. However, co-morbid conditions such as traumatic brain injury, severe pain, obtunded state, and sedative medications among others may interfere with clinical assessment in the acute stage of injury. In selected patients, MRI thus plays a crucial role in diagnosing and characterizing the extent of spinal trauma. As a complement to CT, MRI is most useful when further imaging characterization for spinal stability and/or neural element compromise is needed. MRA and vessel wall imaging techniques may also be indicated for diagnosing blunt traumatic cerebrovascular injury when CTA findings are equivocal[10].

A-P-C: A PRACTICAL APPROACH TO MRI EVALUATION FOR SPINAL TRAUMA

In this section we introduce an algorithmic approach to MRI interpretation for subaxial spine trauma while highlighting key MRI sequences and findings for each of 3 anatomic spine regions. Readers are referred to other excellent reviews for traumatic injuries of the craniocervical junction[11]. As a framework, this algorithmic approach to subaxial spine trauma incorporates nomenclature and concepts from the AOSpine thoracolumbar injury classification (TLICS)[12] and AOSpine subaxial cervical spine injury models[13] (Table 1). While no classification system for spinal injury has gained universal acceptance, the AOSpine classification systems have become increasingly utilized for their high interrater reliability, relative simplicity, and ease of clinical application. For assessment of stability, the spinal column is divided into anterior and posterior tension bands with an intervening spinal canal and its contents. Type A injuries primarily include vertebral body compression fractures. Type B injuries involve disruption of either the anterior or posterior tension band and are generally considered unstable. Type C injuries are unstable and involve disruption of both anterior and posterior tension bands with associated traumatic distraction or translational injuries of the spine.

(*A*)nterior Tension Band (ATB)—The ATB is composed of the vertebral bodies and intervertebral discs. Important ligaments stabilizing the ATB also include the anterior and posterior longitudinal ligaments. Traumatic injuries to the ATB are best evaluated with FS T2W sequences, preferably with Dixon or short tau inversion recovery (STIR) techniques for fat suppression. Prevertebral fluid and hemorrhage are readily identified with FS T2W imaging and absence of prevertebral fluid in the acute stage of injury virtually excludes an unstable ATB injury[14]. When pre-vertebral fluid is identified, a careful

interrogation of anterior ligamentous structures for traumatic disruption is necessary (Fig 1). With hyperextension injuries, there is potential for unstable ATB distraction and resultant disruption of the ALL, PLL, and intervertebral disc (Fig 1). A partial ATB injury, such as isolated ALL disruption should be described (Fig 2), but does not qualify as an unstable ATB injury according to AOSpine classification[12]. In addition to ligamentous injuries, MRI is also highly sensitive for detection of ATB vertebral compression fractures, including very mild compression injuries with minimal or no vertebral body height loss which may be occult on CT (Fig 3). More severe ATB vertebral body injury with hyperflexion injuries, such as flexion teardrop and burst compression injuries are readily diagnosed with CT. In these cases, MRI complements CT in evaluation of the spinal canal for spinal canal compromise, SCI and for evaluation of potential concomitant posterior tension band ligamentous injuries (Fig 4).

(*P*)osterior Tension Band (PTB)—The PTB similarly includes both osseous and ligamentous components. The posterior elements of each vertebra define the bony contribution while the ligamentum flavum (LF), interspinous ligament (ISL), supraspinous ligament (SL), and facet joint capsules constitute the "posterior ligamentous complex" (PLC), the primary soft tissue stabilizers of the PTB. As with the ATB, initial evaluation of the PTB begins with sagittal FS T2W imaging. Unstable PTB injuries may involve transverse fracture across the bony posterior elements, often as part of a Chance type hyperflexion injury which is readily diagnosed on CT (Fig 5). Alternatively, PTB disruption can involve the soft tissue PLC. MRI plays a critical role in diagnosing unstable PLC disruptions. Because the LF is known to be one of the final structures to tear in predictable PLC injury sequence, close attention to LF integrity is key to determining unstable PLC injury[15] (Fig 6). T2 hyperintensity along the LF without clear disruption of the ligament suggests partial tear or sprain. Definite unstable LF disruption should include unambiguous focal disruption of the ligament with intervening T2 hyperintensity (Fig 6). High resolution T2-weighted imaging without fat suppression, such as 3D T2 SPACE, can be a very useful sequence to complement FS T2W imaging for detailed anatomic delineation of the LF (Fig 6).

(*C*)anal and Contents—MRI in spine trauma is arguably of most value for its exquisite evaluation of the spinal canal and its contents, namely the SC and spinal nerve roots. In patients presenting with clinical signs of acute SC or nerve root injury, determination of SC and/or cauda equina compression is the primary focus of the MRI examination in preparation for emergent surgical decompression. The most frequent etiologies for traumatic spinal canal compromise include herniated disc, bony retropulsion, traumatic spinal malalignment, and extra-arachnoid subdural and epidural space hemorrhages[3]. Pre-existing degenerative spondylosis is also a common cause of spinal canal compromise and predisposing risk factor for acute SCI after even mild trauma, particularly common in the elderly population.

The most studied and validated MRI sequence for SC evaluation is T2W imaging. Axial and sagittal depictions of spinal cord contusion provide complementary information for injury characterization. Schaefer et al. first described a sagittal injury classification system

based on the relative length of intramedullary T2 hyperintensity and presence or absence of intramedullary blood products[16] (Fig 7). Hemorrhage within contusion injury is defined as circumscribed T2 hypointense foci, often involving central gray matter, related to paramagnetic effects of iron from blood products in the form of deoxyhemoglobin and hemosiderin. Axial-based T2W classification of contusion injury at the epicenter using the BASIC score has also been shown to strongly correlate with initial injury severity and neurologic outcome[17] (Fig 7). In a large meta-analysis, Fehlings et al. concluded that MR evidence of intramedullary hemorrhage was the MRI biomarker most strongly associated with injury severity and outcome in acute SCI[18]. In summary, review of axial and sagittal T2W sequences should focus on levels of SC compression, the cranio-caudal and transverse extent of SCI, along with the presence or absence of hemorrhage within the contusion injury.

MRI for Atraumatic Compressive Myelopathy

Compressive myelopathy is a potentially devastating but treatable clinical syndrome of neurologic deficits resulting from SC compression. Patients present clinically with cardinal features of symmetric extremity weakness, urinary retention or incontinence, and a circumferential sensory level which may assist in spatially localizing the level of compressive pathology[19]. In most patients, the spinal cord terminates at the L1-L2 vertebral level and lesions compromising the spinal canal below this level may present with a cauda equina syndrome (CES) related to nerve root compression, which includes saddle paresthesia, bowel, bladder, and sexual dysfunction. MRI is the initial modality of choice for suspected atraumatic compressive myelopathy and CES. The imaging protocol should include a total spine survey with inclusion of FS T2, T1 Pre-contrast, T1 post-contrast and DWI sequences. Dedicated axial imaging may be prescribed based on the sagittal survey or obtained automatically for the entire spine depending on institutional workflow. Knowledge of patient's clinical context is of paramount importance for informing image interpretation. Key risk factors include known malignancy, immunocompromised state, history of intravenous drug use, and use of blood thinning medications. The most common causes of atraumatic compressive myelopathy include extra-arachnoid fluid collections such as epidural abscess and hematoma, degenerative spondylosis, spinal tumors, and spinal webs or adhesions. The MRI-based differential diagnosis begins with determination of the location of offending pathology to either the extra-medullary extra-dural space or extramedullary intradural space (Table 2).

EXTRA-DURAL COMPRESSIVE PATHOLOGY

Spine Infection—Clinical signs and symptoms of spinal infection are often nonspecific, thus highlighting the critical role for MRI in confirming or excluding a suspected diagnosis[20]. Emergent MRI is indicated in patients with new or worsening neurologic deficits coupled with clinical suspicion for infection. Notable risk factors include provided clinical history of sepsis, immunosuppression, recent spinal instrumentation such as surgery or percutaneous spinal procedure, and IV drug abuse in patients with back pain and myelopathy. Leukocytosis may be absent. Elevations in erythrocyte sedimentation rate (ESR) and C-Reactive Protein (CRP), while nonspecific, are frequently observed with spinal infection[21].

Myelopathy from spine infection most frequently relates to mechanical compression of the spinal cord by spinal epidural abscess (SEA) or infectious phlegmon, but secondary SC ischemia and vasculitic infarction have also been implicated[19]. Spinal deformity, such as severe kyphosis related to infectious vertebral and discoligamentous destruction, may also contribute to spinal canal compromise and SC or cauda equina compression. Pyogenic spinal infections are most common in the United States, with *Staphylococcus aureus* accounting for 70% of cases[22]. Arterial hematogenous seeding of the spine is the most common route of spinal contamination. The unique vascular supply of the spine, with each segmental spinal artery supplying adjacent vertebral endplates and subchondral marrow space, accounts for the characteristic pattern of discitis osteomyelitis centered at the intervertebral disc level.

As with MRI features of abscess in other parts of the body, MRI of the spine in the setting of epidural abscess reveals a focal fluid collection in the epidural space with peripheral enhancement and central T2 hyperintensity (Fig 8). DWI may be useful for confirming reduced apparent diffusion coefficient (ADC) measures centrally within the epidural collection consistent with purulent contents[23] (Fig 8). Compressive myelopathy may also result from exuberant epidural phlegmon, without frank abscess. In such cases, solid epidural soft tissue enhancement is present without rim-enhancing fluid collection[21] (Fig 9). Spinal epidural abscess (SEA) is associated with a primary discitis-osteomyelitis (DOM) in more than 80% of cases[24]. Associated findings of adjacent discitis osteomyelitis thus help confirm the diagnosis. In the absence of imaging findings suggestive of associated DOM, or other primary musculoskeletal spinal infection such as adjacent septic facet arthritis or septic costovertebral arthritis, alternative diagnostic considerations should be also considered as isolated epidural abscess without primary musculoskeletal spinal infection is rare[25].

Vertebral osteomyelitis with involvement of multiple non-adjacent vertebral bodies (skip lesions) and relative preservation of the disc space is more characteristic of tuberculous spondylitis[26]. TS is a granulomatous bacterial infection caused by *Mycobacterium tuberculosis* that often presents with a more insidious and chronic clinical presentation compared with pyogenic DOM[21,25,26]. Thoracolumbar spinal involvement is most common and the natural history of this disease includes vertebral body collapse, kyphotic deformity, and resulting Gibbus deformity with potential cord compression due both to kyphosis and granulation tissue/bony retropulsion into the epidural space. Contiguous paravertebral and epidural phlegmon and abscess may also be seen in the setting of tuberculosis infection with anterior subligamentous extension of infection aiding in distinction from pyogenic DOM[26] (Fig 10). Intramedullary spinal infections are rare and will be considered separately in more detail in the section covering non-compressive myelopathies.

Neoplasm—Metastases are the most common symptomatic tumors of the spinal column[27]. Spinal metastases may spread hematogenously into the epidural space, but more commonly, epidural spread is via direct extension of tumor from primary osseous spinal or paraspinous sites. Primary neoplasms arising in the epidural space are exceedingly rare and include angiolipoma, lymphoma, and sarcoma. Multiple myeloma is the most common primary bone malignancy to present with compressive myelopathy[27].

In the setting of spinal metastatic disease with emergent clinical presentation, MRI is indicated for identifying levels of epidural tumor encroachment and spinal canal compromise (Fig 11). Assessment for neoplasm related spinal instability should also be addressed in the diagnostic interpretation of the MRI. The *spine instability neoplastic score* (SINS) is a simple point-based scoring system that incorporates many MRI features of spinal involvement to determine an overall risk of malignancy related instability[28]. The Bilsky *epidural spinal cord compression* (ESCC) scale is also a standardized classification system for reporting spinal canal compromise related to spinal metastatic disease[29]. Because medical oncologists, radiation oncologists, and spinal surgeons use these systems to plan patient management, familiarity with and incorporation of these classifications in the MRI interpretation for patients with spinal tumors will enhance timely and appropriate care for patients.

Other extradural compressive pathologies—In the absence of primary spinal column infection, non-infectious etiologies for isolated epidural fluid collection should be considered, the most common of which is epidural hematoma (EDH). Nontraumatic EDHs typically result from venous plexus hemorrhage in the setting of anticoagulation or coagulopathy[30]. Acute hemorrhage in the epidural space characteristically presents as a T1 isointense or hyperintense and T2 hyperintense collection that subtends the dura[30] (Fig 12). The uplifted dura can be seen as a hypointense membrane containing the hematoma on T2W imaging (Fig 12). In the absence of findings suggestive of underlying spinal vascular pathology, such as dilated pial vessel flow voids or enhancing vascular nidus, conventional digital subtraction angiography is likely not necessary for further workup[31]. When there is SC compression and clinical evidence of myelopathy, emergent surgical decompression is indicated.

Cervical spondylotic myelopathy is the most common cause of spinal injury in the United States and is a general term for compression of the spinal cord due to degenerative spinal canal compromise and cord compression[32]. These changes may include disc pathology such as herniation and disc osteophyte complex formation, but also spondylolisthesis, ossification of the posterior longitudinal ligament or ligamentum flavum, and facet arthropathy are frequently implicated. MRI features suggestive of spondylotic myelopathy include variably extensive spinal cord T2 hyperintensity with edema centered in the central gray matter and associated short segment area of pancakelike transverse white matter contrast enhancement centered at the level of maximal cord compression[33] (Fig 13). More acute spondylotic myelopathy may lack associated enhancement.

INTRA-DURAL COMPRESSIVE PATHOLOGY

Extramedullary intradural masses arise within the subarachnoid space, but are separate from the spinal cord. Most frequently encountered examples include metastatic and primary tumors as well as developmental cystic lesions, such as dermoid, epidermoid, arachnoid, and neurenteric cysts. Metastatic tumors in this location are most frequently the result of leptomeningeal spread in the setting of widely disseminated lung, breast, melanoma, gastrointestinal, or hematologic malignancies, although primary brain neoplasms may also produce intrathecal "drop metastases" to the spine.

The most common extramedullary intradural primary tumors are meningioma, nerve sheath tumor, and lipoma, while malignant peripheral nerve sheath tumor, solitary fibrous tumor/hemangiopericytoma, and paragangliomas are additional more rare considerations[34]. Evaluating the MRI signal characteristics of extramedullary intradural masses may help narrow the diagnosis. For instance, schwannomas and neurofibromas are more likely than meningiomas to expand and remodel the neural foramen and may exhibit a characteristic dumbbell morphology with transforaminal extension along the proximal nerve root course[34]. Like their intracranial counterparts, meningiomas will demonstrate broad dural attachment and often follow the signal of grey matter on T1W and T2W imaging and enhance avidly and homogeneously (Fig 14). Evidence of tumor mineralization on CT or T2*-weighted MRI also favors meningioma[24].

Spinal arachnoid cysts may be difficult to distinguish from spinal canal webs and SC herniations, as all of these lesions tend to displace the spinal cord ventrally. When an arachnoid cyst is suspected, high resolution 3D T2 or FIESTA imaging sequences of the spine may be useful to resolve thin cyst walls and confirm the diagnosis[35]. The distortion of the spinal cord seen in the setting of arachnoid web or spinal cord herniation tends to be more focal than that seen with an arachnoid cyst. In the setting of arachnoid webs, there is characteristic focal ventral displacement of the cord with asymmetric posterior cord indentation resembling the profile of the blade of a scalpel (i.e. scalpel sign)[36] (Fig 15). This imaging feature is useful in distinguishing from the ventrally tethered spinal cord observed in the setting of cord herniation where the posterior spinal indentation is more symmetric in the craniocaudal axis. With both spinal webs and herniations, there may be associated intramedullary T2 hyperintensity within the cord and syrinx or pre-syrinx formation in severe cases.

MRI for Noncompressive Spine Emergencies

Noncompressive myelopathy encompasses a vast array of neurological disorders related to intrinsic spinal cord pathology. This includes infectious, inflammatory, and autoimmune diseases, vascular, neoplastic, toxic-metabolic injury, radiation injury, and idiopathic conditions. MRI of the spine in these cases is critically important for characterization of the involved areas in both the axial and sagittal dimensions. Distinct patterns of axial spinal cord involvement can help focus a differential diagnosis and include long segment centromedullary, grey matter/frontal horn predominant, eccentric white matter, patchy irregular, and extramedullary distributions[37,38] (Table 3). Sagittal spinal cord involvement can be described as either longitudinal extensive, spanning at least three sequential vertebral bodies, or short-segment. While patterns of spinal cord involvement can directly inform the differential diagnosis, it is important to recognize that there is substantial overlap between etiologies with each of these patterns. In addition to grouping by location and extent, causes of non-compressive myelopathy can also be categorized into inflammatory and non-inflammatory causes[20]. In clinical practice, suspicion for an infectious or inflammatory etiology may be raised by leukocytosis or elevated serum ESR and CRP levels, elevated WBC, elevated CSF protein, or the presence of immunoglobulins or oligoclonal bands in CSF[20].

INFECTIOUS, PARAINFECTIOUS, AND INFLAMMATORY MYELITIS

Primary infections of the spinal cord are fortunately rare, yet critically important due to high associated mortality and morbidity. Causes include viral, bacterial, parasitic, and fungal pathogens[20]. Early recognition and diagnosis are important so immediate antimicrobial therapy can be initiated. Some infections are more common in immune-compromised individuals, and the immune status of the patient should be determined in order to provide the most relevant differential diagnosis. Additional risk factors such as recent travel and IV drug abuse history should be ascertained.

Certain pathogens have characteristic patterns of involvement related to tropism, such as the anterior horn involvement typical of poliovirus, enteroviruses, and West Nile Virus (WNV)[39,40]. Acute frontal horn infections can result in the clinical syndrome of acute flaccid myelitis (AFM) characterized by sudden weakness in the extremities and loss of reflexes. While poliovirus has been largely eradicated, there has been increased recognition of enterovirus A71 and D68 subtypes as the most common causes of modern AFM[39]. Biennial outbreaks of AFM in the Western United States dating back to 2014 have raised awareness of this disease. The majority of cases involve children with a median age of 6 years[41]. The associated radiologic pattern of frontal horn-predominant long segment T2 hyperintensity aids in diagnosis on spine MRI for patients presenting clinically with rapid-onset flaccid paralysis of one or more limbs and sensory sparing (Fig 16). Gray matter involvement may be unilateral or bilateral and associated ventral nerve rootlet thickening and hyperenhancement is often observed. WNV-associated AFM is exceedingly rare, but shares many imaging features with enteroviral related AFM but is more common in adults[40].

Infectious and postinfectious myelitis presents most often with ellipsoid or patchy long segment centromedullary pattern of spinal cord involvement characteristic of the broad diagnostic category of infectious and non-infectious diseases often grouped under the umbrella term "acute transverse myelitis". Identification of associated nerve root enhancement can be helpful for suggesting an infectious etiology in these cases[37]. Patients present clinically with motor, sensory, and autonomic dysfunction. Primary infectious and postinfectious pathologies with this MRI pattern include cytomegalovirus (CMV), Epstein-Barr virus (EBV), Lyme disease, hepatitis C, parainfectious transverse myelitis (PITM), and acute disseminated encephalomyelitis (ADEM). PITM refers to SCI resulting from a post-infectious immune-mediated response[42]. Preceding infections of viral hepatitis, *Mycoplasma pneumonia*, *Campylobacter jejuni*, CVM, and EBV species among others should trigger consideration of PITM in patients with MRI and clinical features of acute transverse myelitis[42]. There are no pathognomonic imaging characteristics that can reliably identify the causative etiology of PITM, therefore clinical history and laboratory studies are important in confirming a suspected diagnosis.

Noninfectious causes of inflammatory myelitis include autoimmune diseases such as multiple sclerosis (MS), neuromyelitis optica spectrum disorders (NMOSD), and myelin oligodendrocyte glycoprotein antibody disease (MOGAD)[20]. Acute treatment for these disorders in the emergent setting is tailored to suppressing the pathologic immune response with steroids, plasmapheresis, and long-acting immunomodulating therapies when necessary. MRI in the emergent setting plays a central role in diagnosing these disorders

and enabling timely treatment. MS, the most common inflammatory myelitis, is a primary demyelinating disease with white matter predominant involvement. T2-hyperintense MS lesions are typically short segment, spanning less than 2 vertebral segments, and eccentric. Enhancement is observed in the active stages of inflammatory demyelination. Brain imaging is useful to show associated demyelinating plaques of the brain. NMOSD is an antibody-mediated disease of aggressive spinal demyelination and optic neuritis, which classically presents on MRI with long-segment T2 hyperintense spinal edema spanning 3 or more vertebral segments[43] (Fig 17). Centromedullary T2 hyperintensity of the cord with preferential cervical spine involvement and avid contrast enhancement is typical. Oligoclonal bands are not present in NMO, although immunoglobin G targeting aquaporin-4 is a specific marker for this disease.

MOGAD may present with longitudinally extensive as well as multiple short segment lesions. Central gray-matter T2 hyperintensity on axial imaging has been termed the "H" sign of MOGAD myelitis[44]. Post contrast enhancement, when present, is usually faint and patchy and may include linear subependymal enhancement paralleling the central canal. There is a predilection for conus involvement with leptomeningeal and cauda equina enhancement[44].

Other inflammatory causes of myelitis include systemic inflammatory and connective tissue disorders including sarcoidosis, lupus, and Sjögren's disease. Theses systemic diseases may present with a transverse myelitis or an irregular pattern of patchy cord involvement. Spinal lesions may enhance in a patchy distribution, "skipping" adjacent portions of the cord and distinguishing these diseases from intramedullary neoplasms, which tend to be continuous and infiltrative. Pial and subpial infiltrative enhancement along the dorsal cord white matter forming a "trident sign" pattern is highly suggestive of neurosarcoidosis[45] (Fig 18).

VASCULAR SPINE EMERGENCIES

The most common emergent spine vascular pathologies include acute spinal cord infarct, spinal arteriovenous shunts, and hemorrhagic cavernous malformations[46]. The spinal cord has complex arterial collateralization between a single anterior and paired posterior spinal arteries. Lower thoracic spinal cord infarcts of the anterior spinal artery territory are most common due to the relatively limited collateralization for the dominant radicular artery of Adamkiewicz territory[46]. Spinal infarcts occur more frequently in women, with an average age of 56 years[46]. Significant risk factors include recent aortic surgery, embolism, vasculitis, dissection, and hypotension. MRI may aid in diagnosing acute spinal cord infarct in patients presenting with acute onset weakness, sensory changes, and sphincter dysfunction without antecedent trauma or spinal cord compression. MRI signal abnormalities related to acute infarct may be occult for up to 24 hours after symptom onset[47]. Within 2 days, MRI usually reveals long segment ventral spinal cord T2 hyperintensity primarily involving the metabolically active frontal horns, termed the "owl's eye" sign of cord infarction[48] (Fig 19). Associated hyperintensity on DWI with reduced ADC values helps confirm the diagnosis of acute spinal cord infarct. Given the shared vascular supply with vertebral bodies, associated vertebral edema at the same level as the cord infarct can help discern from other pathologies that involve the ventral spinal cord[46] (Fig 19). A less common cause of

cord infarction is termed surfer's myelopathy. Underlying pathophysiology is incompletely understood, but likely relates to extended cervical hyperextension in novice surfers while paddling their surfboards in the prone position and looking forward, resulting in tension on the spinal cord and surrounding vasculature and avulsion of perforating vessels[49]. Other rare etiologies include fibrocartilaginous embolism from herniated disc material and decompression sickness.

Among arteriovenous shunting lesions, dural arteriovenous fistulas (dAVF) are most common, accounting for 60–80% of all spinal vascular lesions[50]. The fistulous point most frequently occurs at the dural sleeve within a neural foramen. Spinal dAVFs are more common in middle-aged and older men with insidious clinical symptoms of lower extremity weakness, sensory changes, and sphincter dysfunction. Longstanding venous hypertension from the fistula contributes to peri-medullary venous engorgement and congestive venous myelopathy of the SC. On MRI, intramedullary spinal cord T2-hyperintense edema with predelection for conus involvement in conjunction with dilated perimedullary vascular flow voids are characteristic MRI features[46] (fig). The cord edema and vascular flow voids may not be located at the same level, and the location of either does not reliably correlate with the location of the fistula. Central cord and cauda equina nerve root enhancement may also be observed. While conventional digital subtraction angiography of the spine is recommended for diagnostic confirmation and potential treatment, time-resolved MRA may aid in identifying the level of fistulous connection in up to 73% of cases[51] (Fig 20). Additional more rare spinal arteriovenous shunts include intramedullary glomus arterovenous malformations (AVMs), metameric AVMs, and perimedullary AVMs.

Spinal cord cavernous malformations exhibit many of the same imaging features as seen with cavernous malformations in the brain. T2-hypointense margins with central T1 and T2 heterogenous signal and marked susceptibility artifact within the spinal cord are characteristic MRI features. There is no arteriovenous shunt, therefore MRI is superior to spDSA for making the diagnosis. Ventral spinal location is a negative prognostic indicator[52].

TOXIC-METABOLIC AND RADIATION-RELATED SPINE EMERGENCIES

The most common toxic-metabolic cause of emergent myelopathy is Vitamin B12-deficiency, which causes pernicious anemia and subacute combined degeneration. This disease may result from parietal cell autoantibodies, insufficient dietary intake of B12, or intrinsic factor deficiency. Clinical symptoms include spastic paraparesis with distal proprioceptive loss, while typical imaging findings include long-segment T2 hyperintensity of the dorsal columns (Fig 20). Associated involvement of the anterolateral columns accounts for the term subacute combined degeneration. Enhancement is unusual. Symptoms and imaging findings may resolve with adequate medical treatment of Vitamin B12 deficiency. Abuse of nitrous oxide, copper deficiency, and zinc toxicity may also cause subacute combined degeneration and thus have identical imaging findings.

Radiation myelopathy can occur either in the immediate aftermath or in a delayed fashion, years after radiation exposure. Radiation myelitis is most often seen after radiation therapy for head and neck cancer and vertebral metastases, usually when patients have received an excess of 4000 rads[53]. Radiation myelopathy may resolve spontaneously

or progress insidiously to spinal atrophy and severe disability and death. There is no effective treatment. Early imaging manifestations are nonspecific and include long-segment centromedullary T2 hyperintensity and patchy enhancement[38]. While spinal cord findings are nonspecific, intrinsic T1 hyperintensity of vertebral bodies corresponding to the radiation field, representing fatty bone marrow replacement, is a useful associated imaging finding to confirm the diagnosis[54] (Fig 21).

INTRAMEDULLARY SPINAL CORD MASSES

Intramedullary spinal cord masses and mass-like lesions vary widely in etiology and imaging appearance. Patients may present with pain, weakness and sensory changes depending on mass location. Etiologies include primary and metastatic tumors, spinal cord abscess, and cavernous malformations as discussed in the prior section on vascular lesions. Masses should be characterized as circumscribed or infiltrative. The most common primary intramedullary neoplasms include ependymoma, astrocytoma, and hemangioblastoma. Ependymomas are the most common spinal glial tumor in adults and arise from the central canal or from cell rests along the filum terminale[55]. As such, they tend to be centrally located in the spinal cord with symmetric expansion and well-circumscribed margins. Tumor cysts may be seen in up to 22% of ependymomas and adjacent syringohydromyelia is common[55]. Intratumoral hemorrhage can lead to hypointense hemosiderin rim on T2W imaging known as the "cap sign"[55] (Fig 22). Avid yet heterogenous tumor enhancement is typical. Astrocytomas are the most common spinal glial tumor in children and are more eccentric, infiltrative, and more likely to involve the entire transverse extent of the cord compared with ependymomas[55] (Fig 22). Hemorrhage is uncommon in astrocytomas. Hemangioblastomas have highly variable MRI appearance, but often involve multiple vertebral levels with avid enhancement. In large tumors, identification of associated prominent vascular flow voids within the tumor should prompt consideration of spinal hemangioblastoma[55] (Fig 22). Hemorrhage is common and the hemosiderin "cap sign" may also be observed. Multiple spinal hemangioblastomas suggests underlying von hippel lindau (VHL) disease.

Intramedullary spinal cord metastases are fortunately rare and clinical history of known widespread malignancy helps favor the diagnosis. On MRI, metastases to the SC are expansile with prominent surrounding edema. Following contrast administration, thin linear rim enhancement with more ill defined enhancement emanating along the superior and inferior margins (rim and flame signs respectively) have been described as characteristic features[56].

Intramedullary spinal abscess is rare and may arise from contiguous or hematogenous spread. Congenital dermal sinus tracts may predispose to the development of intramedullary spinal abscesses, particularly in the pediatric population. These lesions have an MRI appearance similar to intracranial abscesses, with diffuse or rim enhancement, surrounding edema, and reduced diffusion centrally, although early in the course of the disease the only finding may be ill-defined T2-hyperintensity with or without patchy enhancement[57]. Similar to epidural or intracranial abscesses, the most common causative organisms are *Staphylococcus* and *Streptococcus* species[37].

POLYRADICULOPATHIES

Guillain Barre Syndrome (GBS) is an acute, demyelinating polyneuropathy that is often proceeded by a viral illness, although it may also be associated with vaccine administration and autoimmune disorders. There are several subtypes of GBS, including motor and motor-sensory axonal subtypes and regional GBS (Miller-Fisher variant). The diagnosis is suspected in patients presenting with ascending flaccid paralysis. CSF studies reveal elevated protein without leukocytosis. The diagnosis of GBS may be supported or suggested on MRI by smooth enhancement of the cauda equina nerve roots preferentially involving the ventral motor rootlets, although the main purpose of imaging in these patients often serves to exclude other treatable causes of acute paralysis (Fig 22). GBS has recently been reported with COVID-19 related SARS-CoV-2 infection[58]. In a systematic review of 73 patients with GBS associated with COVID-19, neurologic symptoms presented between 2 and 33 days after respiratory symptom onset[59]. Of note, CSF PCR was insensitive and negative for SARS-CoV-2 in all patients tested.

The differential diagnosis for nerve root enhancement is broad and in addition to GBS, includes leptomeningeal carcinomatosis, chronic inflammatory demyelinating polyneuropathy (CIDP), arachnoiditis, sarcoidosis, lymphoma, and infectious radiculitis. Generally, these differential considerations are associated with a nonspecific CSF profile including elevated protien, so clinical presentation and patient history along with imaging findings are usually instrumental in making the final diagnosis. For instance, leptomeningeal carcinomatosis typically occurs in the setting of widespread metastatic disease. Chronic inflammatory demyelinating (CIDP) polyneuropathy is a heterogeneous group of demyelinating polyneuropathies that may be antibody mediated or immune cell mediated; regardless of the specific underlying etiology and pathophysiology, this syndrome is chronic by definition, with symptoms typically progressing over several months. Arachnoiditis refers to inflammation of the nerves and nerve roots and can be caused by a variety of etiologies including infection, prior intradural surgical manipulation, and intrathecal drug administration. Patients with neurosarcoidosis causing leptomeningeal inflammation will usually have other stigmata of this disease, even if the neurologic symptoms are the first manifestation. Primary leptomeningeal lymphoma is a rare form of primary CNS lymphoma and a rare cause of leptomeningeal enhancement; the diagnosis is made by identifying malignant lymphocytes on CSF cytology. Finally, AIDS-associated cytomegalovirus polyradiculopathy and Lyme disease will be associated with specific exposures and/or clinical and laboratory signs of these infections. The radiologist should be prepared to synthesize this clinical data in order to narrow the differential diagnosis.

Conclusion

MRI plays a central role in the timely diagnosis and treatment for spine emergencies. For traumatic emergencies, MRI plays a complementary role to CT. Knowledge of the most up-to-date traumatic spine injury classification systems forms a framework for an algorithmic search pattern to best inform treatment decisions. Diagnostic considerations for atraumatic spine emergencies are broad, and MRI is the first line imaging modality for initially determining whether there is compressive pathology. Familiarity with key MR imaging

findings along with knowledge of relevant clinical history is necessary for diagnosing both compressive and non-compressive atraumatic spine emergencies.

REFERENCES

1. Daffner RH, Hackney DB. ACR Appropriateness Criteria on suspected spine trauma. J Am Coll Radiol. Nov 2007;4(11):762–75. doi:10.1016/j.jacr.2007.08.006 [PubMed: 17964500]

2. Shah LM, Ross JS. Imaging of Spine Trauma. Neurosurgery. Nov 2016;79(5):626–642. doi:10.1227/NEU.0000000000001336 [PubMed: 27404215]

3. Talbott JF, Huie JR, Ferguson AR, Bresnahan JC, Beattie MS, Dhall SS. MR Imaging for Assessing Injury Severity and Prognosis in Acute Traumatic Spinal Cord Injury. Radiol Clin North Am. Mar 2019;57(2):319–339. doi:10.1016/j.rcl.2018.09.004 [PubMed: 30709473]

4. Arce D, Sass P, Abul-Khoudoud H. Recognizing spinal cord emergencies. Am Fam Physician. Aug 15 2001;64(4):631–8. [PubMed: 11529262]

5. Expert Panel on Neurological I, Hutchins TA, Peckham M, et al. ACR Appropriateness Criteria(R) Low Back Pain: 2021 Update. J Am Coll Radiol. Nov 2021;18(11S):S361–S379. doi:10.1016/j.jacr.2021.08.002 [PubMed: 34794594]

6. Mirowitz SA, Heiken JP, Brown JJ. Evaluation of fat saturation technique for T2-weighted endorectal coil MRI of the prostate. Magn Reson Imaging. 1994;12(5):743–7. doi:10.1016/0730-725x(94)92199-7 [PubMed: 7934661]

7. Lammertse D, Dungan D, Dreisbach J, et al. Neuroimaging in traumatic spinal cord injury: an evidence-based review for clinical practice and research. J Spinal Cord Med. 2007;30(3):205–14. [PubMed: 17684886]

8. Shanmuganathan K, Zhuo J, Chen HH, et al. Diffusion Tensor Imaging Parameter Obtained during Acute Blunt Cervical Spinal Cord Injury in Predicting Long-Term Outcome. J Neurotrauma. Nov 1 2017;34(21):2964–2971. doi:10.1089/neu.2016.4901 [PubMed: 28385062]

9. Kurpad S, Martin AR, Tetreault LA, et al. Impact of Baseline Magnetic Resonance Imaging on Neurologic, Functional, and Safety Outcomes in Patients With Acute Traumatic Spinal Cord Injury. Global Spine J. Sep 2017;7(3 Suppl):151S–174S. doi:10.1177/2192568217703666 [PubMed: 29164022]

10. Vranic JE, Huynh TJ, Fata P, et al. The ability of magnetic resonance black blood vessel wall imaging to evaluate blunt cerebrovascular injury following acute trauma. J Neuroradiol. May 2020;47(3):210–215. doi:10.1016/j.neurad.2019.01.091 [PubMed: 30677426]

11. Riascos R, Bonfante E, Cotes C, Guirguis M, Hakimelahi R, West C. Imaging of Atlanto-Occipital and Atlantoaxial Traumatic Injuries: What the Radiologist Needs to Know. Radiographics. Nov-Dec 2015;35(7):2121–34. doi:10.1148/rg.2015150035 [PubMed: 26562241]

12. Vaccaro AR, Oner C, Kepler CK, et al. AOSpine thoracolumbar spine injury classification system: fracture description, neurological status, and key modifiers. Spine (Phila Pa 1976). Nov 1 2013;38(23):2028–37. doi:10.1097/BRS.0b013e3182a8a381 [PubMed: 23970107]

13. Vaccaro AR, Koerner JD, Radcliff KE, et al. AOSpine subaxial cervical spine injury classification system. Eur Spine J. Jul 2016;25(7):2173–84. doi:10.1007/s00586-015-3831-3 [PubMed: 25716661]

14. Henninger B, Kaser V, Ostermann S, et al. Cervical Disc and Ligamentous Injury in Hyperextension Trauma: MRI and Intraoperative Correlation. J Neuroimaging. Jan 2020;30(1):104–109. doi:10.1111/jon.12663 [PubMed: 31498526]

15. Pizones J, Izquierdo E, Sanchez-Mariscal F, Zuniga L, Alvarez P, Gomez-Rice A. Sequential damage assessment of the different components of the posterior ligamentous complex after magnetic resonance imaging interpretation: prospective study 74 traumatic fractures. Spine (Phila Pa 1976). May 15 2012;37(11):E662–7. doi:10.1097/BRS.0b013e3182422b2b [PubMed: 22146288]

16. Schaefer DM, Flanders A, Northrup BE, Doan HT, Osterholm JL. Magnetic resonance imaging of acute cervical spine trauma. Correlation with severity of neurologic injury. Spine (Phila Pa 1976). Oct 1989;14(10):1090–5. [PubMed: 2588058]

17. Talbott JF, Whetstone WD, Readdy WJ, et al. The Brain and Spinal Injury Center score: a novel, simple, and reproducible method for assessing the severity of acute cervical spinal cord injury with axial T2-weighted MRI findings. J Neurosurg Spine. Oct 2015;23(4):495–504. doi:10.3171/2015.1.SPINE141033 [PubMed: 26161519]

18. Fehlings MG, Martin AR, Tetreault LA, et al. A Clinical Practice Guideline for the Management of Patients With Acute Spinal Cord Injury: Recommendations on the Role of Baseline Magnetic Resonance Imaging in Clinical Decision Making and Outcome Prediction. Global Spine J. Sep 2017;7(3 Suppl):221S–230S. doi:10.1177/2192568217703089 [PubMed: 29164028]

19. Ropper AE, Ropper AH. Acute Spinal Cord Compression. N Engl J Med. Apr 6 2017;376(14):1358–1369. doi:10.1056/NEJMra1516539 [PubMed: 28379788]

20. Douglas AG, Xu DJ, Shah MP. Approach to Myelopathy and Myelitis. Neurol Clin. Feb 2022;40(1):133–156. doi:10.1016/j.ncl.2021.08.009 [PubMed: 34798966]

21. Talbott JF, Shah VN, Uzelac A, et al. Imaging-Based Approach to Extradural Infections of the Spine. Semin Ultrasound CT MR. Dec 2018;39(6):570–586. doi:10.1053/j.sult.2018.09.003 [PubMed: 30527522]

22. Hadjipavlou AG, Mader JT, Necessary JT, Muffoletto AJ. Hematogenous pyogenic spinal infections and their surgical management. Spine (Phila Pa 1976). Jul 1 2000;25(13):1668–79. [PubMed: 10870142]

23. Dumont RA, Keen NN, Bloomer CW, et al. Clinical Utility of Diffusion-Weighted Imaging in Spinal Infections. Clin Neuroradiol. Mar 26 2018;doi:10.1007/s00062-018-0681-5

24. Lavi ES, Pal A, Bleicher D, Kang K, Sidani C. MR Imaging of the Spine: Urgent and Emergent Indications. Semin Ultrasound CT MR. Dec 2018;39(6):551–569. doi:10.1053/j.sult.2018.10.006 [PubMed: 30527521]

25. Go JL, Rothman S, Prosper A, Silbergleit R, Lerner A. Spine infections. Neuroimaging Clin N Am. Nov 2012;22(4):755–72. doi:10.1016/j.nic.2012.06.002 [PubMed: 23122265]

26. Torres C, Zakhari N. Imaging of Spine Infection. Semin Roentgenol. Jan 2017;52(1):17–26. doi:10.1053/j.ro.2016.05.013 [PubMed: 28434499]

27. Gibbs WN, Nael K, Doshi AH, Tanenbaum LN. Spine Oncology: Imaging and Intervention. Radiol Clin North Am. Mar 2019;57(2):377–395. doi:10.1016/j.rcl.2018.10.002 [PubMed: 30709476]

28. Fisher CG, DiPaola CP, Ryken TC, et al. A novel classification system for spinal instability in neoplastic disease: an evidence-based approach and expert consensus from the Spine Oncology Study Group. Spine (Phila Pa 1976). Oct 15 2010;35(22):E1221–9. doi:10.1097/BRS.0b013e3181e16ae2 [PubMed: 20562730]

29. Bilsky MH, Laufer I, Fourney DR, et al. Reliability analysis of the epidural spinal cord compression scale. J Neurosurg Spine. Sep 2010;13(3):324–8. doi:10.3171/2010.3.SPINE09459 [PubMed: 20809724]

30. Braun P, Kazmi K, Nogues-Melendez P, Mas-Estelles F, Aparici-Robles F. MRI findings in spinal subdural and epidural hematomas. Eur J Radiol. Oct 2007;64(1):119–25. doi:10.1016/j.ejrad.2007.02.014 [PubMed: 17353109]

31. Lonjon MM, Paquis P, Chanalet S, Grellier P. Nontraumatic spinal epidural hematoma: report of four cases and review of the literature. Neurosurgery. Aug 1997;41(2):483–6; discussion 486–7. doi:10.1097/00006123-199708000-00035 [PubMed: 9257319]

32. Onofrei LV, Henrie AM. Cervical and Thoracic Spondylotic Myelopathies. Semin Neurol. Jun 2021;41(3):239–246. doi:10.1055/s-0041-1725144 [PubMed: 34010970]

33. Flanagan EP, Marsh RW, Weinshenker BG. Teaching neuroimages: "pancake-like" gadolinium enhancement suggests compressive myelopathy due to spondylosis. Neurology. May 21 2013;80(21):e229. doi:10.1212/WNL.0b013e318293e346 [PubMed: 23690303]

34. Koeller KK, Shih RY. Intradural Extramedullary Spinal Neoplasms: Radiologic-Pathologic Correlation. Radiographics. Mar-Apr 2019;39(2):468–490. doi:10.1148/rg.2019180200 [PubMed: 30844353]

35. Li Z, Chen YA, Chow D, Talbott J, Glastonbury C, Shah V. Practical applications of CISS MRI in spine imaging. Eur J Radiol Open. 2019;6:231–242. doi:10.1016/j.ejro.2019.06.001 [PubMed: 31304197]

36. Reardon MA, Raghavan P, Carpenter-Bailey K, et al. Dorsal thoracic arachnoid web and the "scalpel sign": a distinct clinical-radiologic entity. AJNR Am J Neuroradiol. May 2013;34(5):1104–10. doi:10.3174/ajnr.A3432 [PubMed: 23348759]

37. Talbott JF, Narvid J, Chazen JL, Chin CT, Shah V. An Imaging-Based Approach to Spinal Cord Infection. Semin Ultrasound CT MR. Oct 2016;37(5):411–30. doi:10.1053/j.sult.2016.05.006 [PubMed: 27616314]

38. Lee MJ, Aronberg R, Manganaro MS, Ibrahim M, Parmar HA. Diagnostic Approach to Intrinsic Abnormality of Spinal Cord Signal Intensity. Radiographics. Oct 2019;39(6):1824–1839. doi:10.1148/rg.2019190021 [PubMed: 31589577]

39. Messacar K, Schreiner TL, Maloney JA, et al. A cluster of acute flaccid paralysis and cranial nerve dysfunction temporally associated with an outbreak of enterovirus D68 in children in Colorado, USA. Lancet. Apr 25 2015;385(9978):1662–71. doi:10.1016/S0140-6736(14)62457-0 [PubMed: 25638662]

40. Kraushaar G, Patel R, Stoneham GW. West Nile Virus: a case report with flaccid paralysis and cervical spinal cord: MR imaging findings. AJNR Am J Neuroradiol. Jan 2005;26(1):26–9. [PubMed: 15661693]

41. Ayers T, Lopez A, Lee A, et al. Acute Flaccid Myelitis in the United States: 2015–2017. Pediatrics. Nov 2019;144(5)doi:10.1542/peds.2019-1619

42. Beh SC, Greenberg BM, Frohman T, Frohman EM. Transverse myelitis. Neurol Clin. Feb 2013;31(1):79–138. doi:10.1016/j.ncl.2012.09.008 [PubMed: 23186897]

43. Wingerchuk DM, Banwell B, Bennett JL, et al. International consensus diagnostic criteria for neuromyelitis optica spectrum disorders. Neurology. Jul 14 2015;85(2):177–89. doi:10.1212/WNL.0000000000001729 [PubMed: 26092914]

44. Dubey D, Pittock SJ, Krecke KN, et al. Clinical, Radiologic, and Prognostic Features of Myelitis Associated With Myelin Oligodendrocyte Glycoprotein Autoantibody. JAMA Neurol. Mar 1 2019;76(3):301–309. doi:10.1001/jamaneurol.2018.4053 [PubMed: 30575890]

45. Zalewski NL, Krecke KN, Weinshenker BG, et al. Central canal enhancement and the trident sign in spinal cord sarcoidosis. Neurology. Aug 16 2016;87(7):743–4. doi:10.1212/WNL.0000000000002992 [PubMed: 27527540]

46. McEntire CR, Dowd RS, Orru E, et al. Acute Myelopathy: Vascular and Infectious Diseases. Neurol Clin. May 2021;39(2):489–512. doi:10.1016/j.ncl.2021.01.011 [PubMed: 33896530]

47. Alblas CL, Bouvy WH, Lycklama ANGJ, Boiten J. Acute spinal-cord ischemia: evolution of MRI findings. J Clin Neurol. Sep 2012;8(3):218–23. doi:10.3988/jcn.2012.8.3.218 [PubMed: 23091532]

48. Weidauer S, Nichtweiss M, Lanfermann H, Zanella FE. Spinal cord infarction: MR imaging and clinical features in 16 cases. Neuroradiology. Oct 2002;44(10):851–7. doi:10.1007/s00234-002-0828-5 [PubMed: 12389137]

49. Freedman BA, Malone DG, Rasmussen PA, Cage JM, Benzel EC. Surfer's Myelopathy: A Rare Form of Spinal Cord Infarction in Novice Surfers: A Systematic Review. Neurosurgery. May 2016;78(5):602–11. doi:10.1227/NEU.0000000000001089 [PubMed: 27082966]

50. Jellema K, Tijssen CC, van Gijn J. Spinal dural arteriovenous fistulas: a congestive myelopathy that initially mimics a peripheral nerve disorder. Brain. Dec 2006;129(Pt 12):3150–64. doi:10.1093/brain/awl220 [PubMed: 16921175]

51. Lee J, Lim YM, Suh DC, Rhim SC, Kim SJ, Kim KK. Clinical presentation, imaging findings, and prognosis of spinal dural arteriovenous fistula. J Clin Neurosci. Apr 2016;26:105–9. doi:10.1016/j.jocn.2015.06.030 [PubMed: 26765752]

52. Liang JT, Bao YH, Zhang HQ, Huo LR, Wang ZY, Ling F. Management and prognosis of symptomatic patients with intramedullary spinal cord cavernoma: clinical article. J Neurosurg Spine. Oct 2011;15(4):447–56. doi:10.3171/2011.5.SPINE10735 [PubMed: 21740129]

53. Marcus RB, Jr., Million RR. The incidence of myelitis after irradiation of the cervical spinal cord. Int J Radiat Oncol Biol Phys. Jul 1990;19(1):3–8. doi:10.1016/0360-3016(90)90126-5 [PubMed: 2380091]

54. Khan M, Ambady P, Kimbrough D, et al. Radiation-Induced Myelitis: Initial and Follow-Up MRI and Clinical Features in Patients at a Single Tertiary Care Institution during 20 Years. AJNR Am J Neuroradiol. Aug 2018;39(8):1576–1581. doi:10.3174/ajnr.A5671 [PubMed: 29773568]

55. Koeller KK, Rosenblum RS, Morrison AL. Neoplasms of the spinal cord and filum terminale: radiologic-pathologic correlation. Radiographics. Nov-Dec 2000;20(6):1721–49. doi:10.1148/radiographics.20.6.g00nv151721 [PubMed: 11112826]

56. Rykken JB, Diehn FE, Hunt CH, et al. Rim and flame signs: postgadolinium MRI findings specific for non-CNS intramedullary spinal cord metastases. AJNR Am J Neuroradiol. Apr 2013;34(4):908–15. doi:10.3174/ajnr.A3292 [PubMed: 23079405]

57. Friess HM, Wasenko JJ. MR of staphylococcal myelitis of the cervical spinal cord. AJNR Am J Neuroradiol. Mar 1997;18(3):455–8. [PubMed: 9090402]

58. Moonis G, Filippi CG, Kirsch CFE, et al. The Spectrum of Neuroimaging Findings on CT and MRI in Adults With COVID-19. AJR Am J Roentgenol. Oct 2021;217(4):959–974. doi:10.2214/AJR.20.24839 [PubMed: 33236647]

59. Abu-Rumeileh S, Abdelhak A, Foschi M, Tumani H, Otto M. Guillain-Barre syndrome spectrum associated with COVID-19: an up-to-date systematic review of 73 cases. J Neurol. Apr 2021;268(4):1133–1170. doi:10.1007/s00415-020-10124-x [PubMed: 32840686]
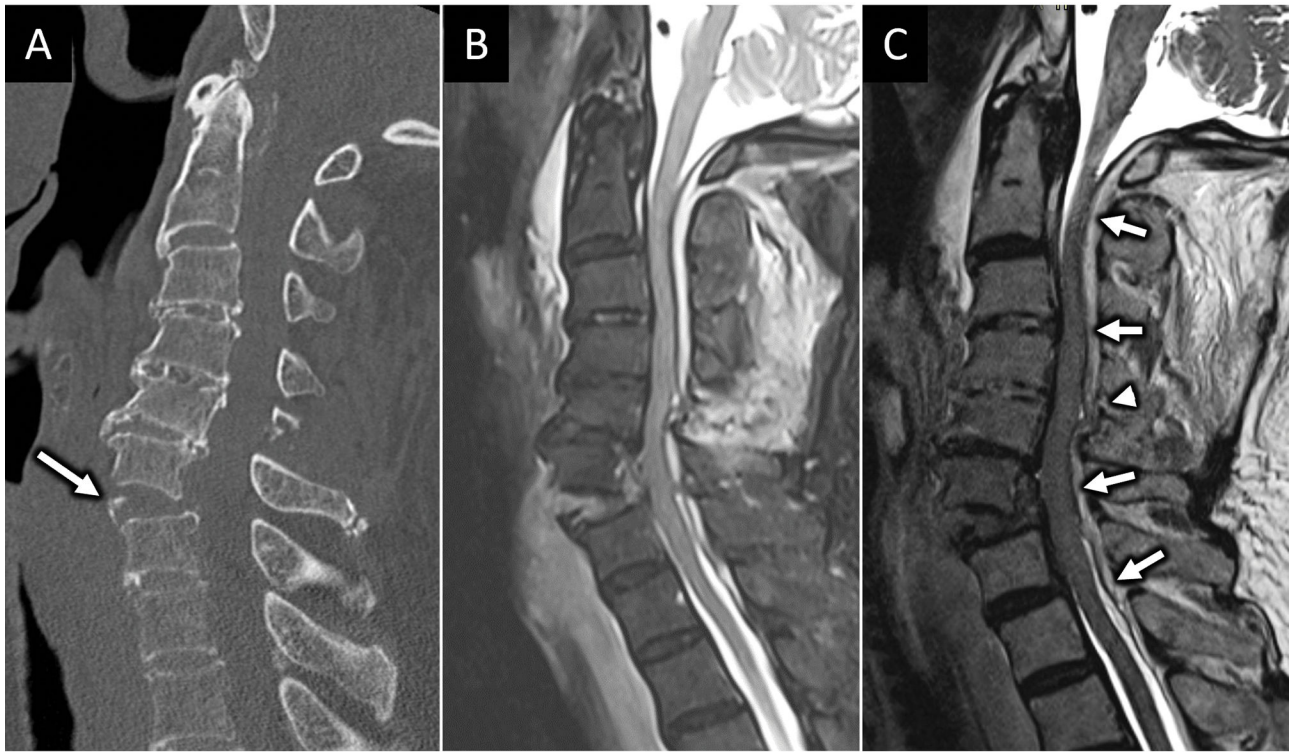
FIGURE 1:
Hyperextension injury with unstable anterior tension band (ATB) disruption. 85-year-old man presents with left sided weakness after ground level fall and headstrike. Sagittal CT image (arrow in A) shows traumatic anterolisthesis at C6-C7 with small anteroinferior avulsion corner fracture of C6 (arrow). Sagittal FS T2W (B) and sagittal T2 SPACE (C) MR images confirm complete disruption of the C6-C7 anterior discoligamentous complex. MRI also reveals long segment severe spinal canal stenosis and cord compression with dorsal epidural hematoma (arrows in C). Focal ligamentum flavum tear at C5–6 is best seen on sagittal T2 SPACE image (arrowhead in C).
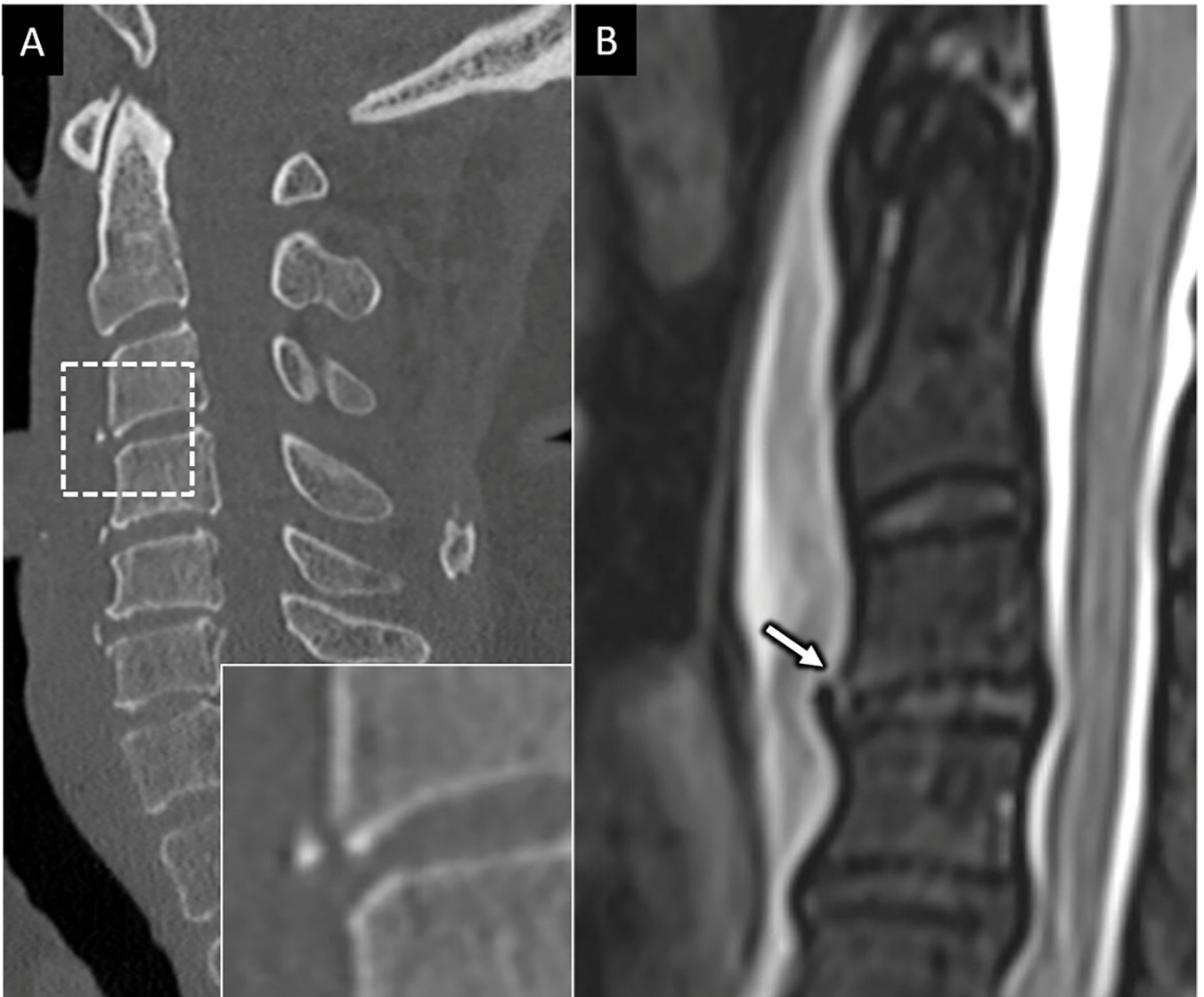
FIGURE 2:

Hyperextension injury with anterior longitudinal ligament (ALL) disruption. 70-year-old female presents with upper extremity paresthesia following low speed pedestrian versus automobile injury. A) Sagittal CT image of the cervical spine shows a small and minimally displaced anteroinferior avulsion corner fracture at C3 (dotted square with zoom in view in the bottom right inset in A). B) Sagittal T2 FS MR imaging of the upper cervical spine in the same patient shows prominent prevertebral fluid collection with focal disruption of the ALL (arrow in B) with otherwise intact anterior discoligamentous complex.
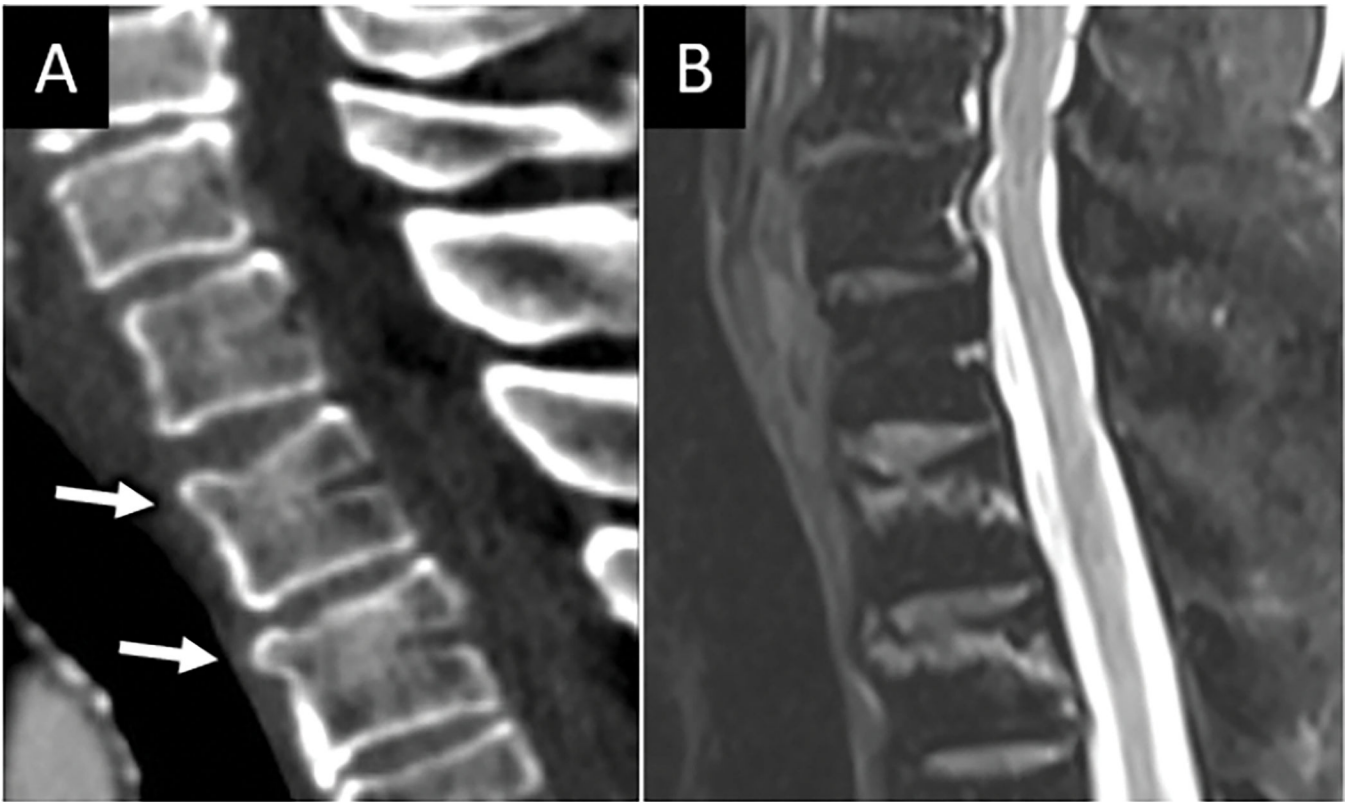
FIGURE 3:
MRI is sensitive for mild vertebral compression injuries. Sagittal CT image (A) in a patient who presented with neck pain after a fall reveals mild superior endplate compression fractures at C6 and C7 (arrows in A), which are easily seen on sagittal T2W MRI (B) where linear subchondral marrow edema underlying the superior endplates conspicuously identifies the acute fractures.
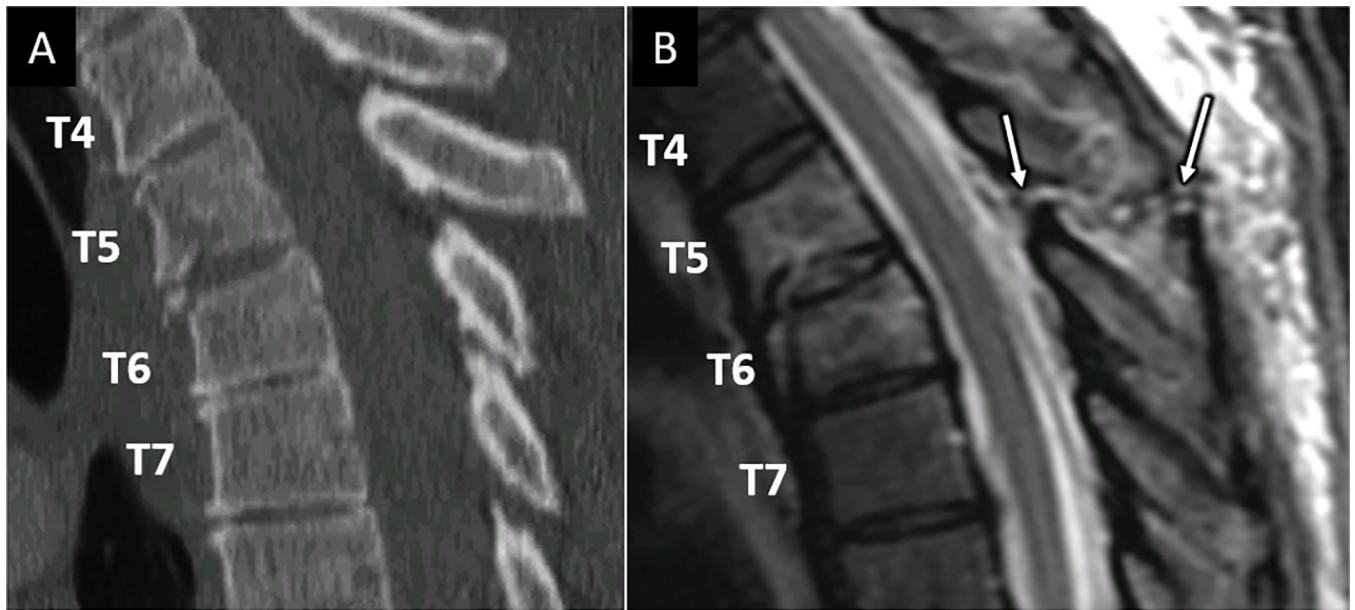
Figure 4:

MRI reveals unsuspected ligamentous posterior tension band disruption. Sagittal CT image (A) for a 48-year-old patient suffering a fall reveals mild anterior compression and endplate fractures at T5 and T6 vertebral levels. Sagittal T2W MR image (B) at the same levels reveals complete disruption of the supraspinous ligament, interspinous ligament, and ligamentum flavum at T5-T6 (arrows in B).
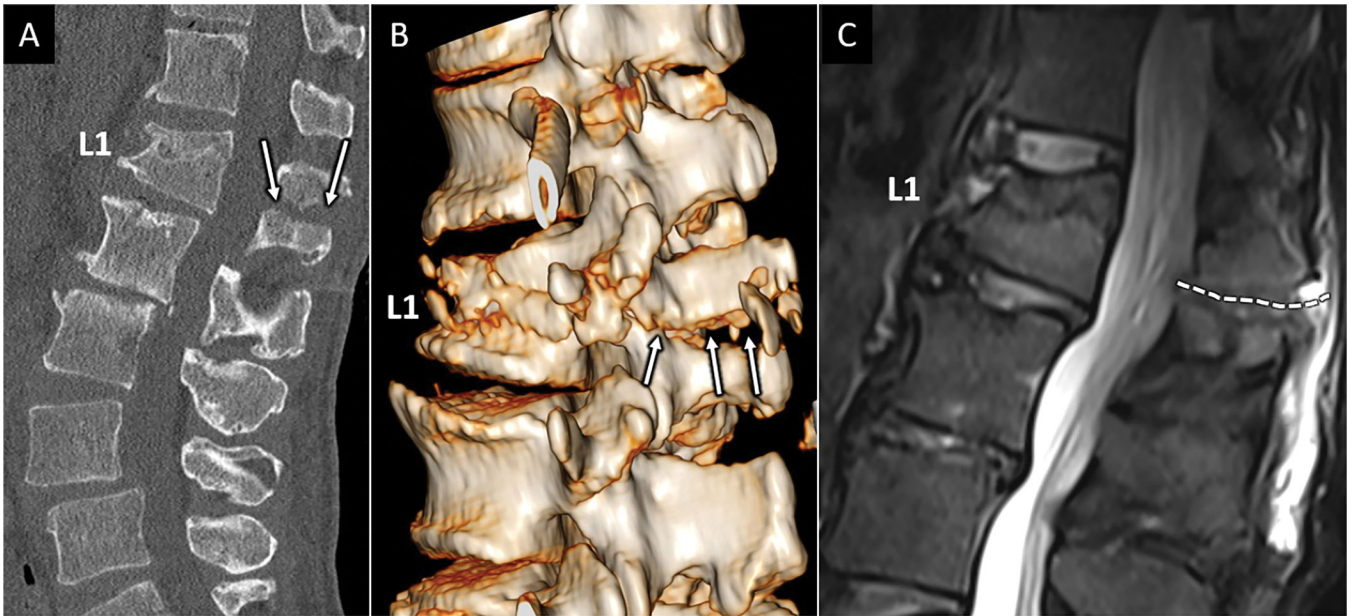
Figure 5:
CT and MRI depictions of Chance fracture. Sagittal CT (A) depicts linear fracture through the spinous process in a 68-year-old female with seatbelt injury and low back pain. B) 3D reconstruction of the CT images clearly depicts transverse fracture through the entire L1 posterior elements (arrows in B) consistent with an AOSpine type B1 injury. Sagittal T2W MR image in the same patient shows marrow edema and transverse distracted fracture line corresponding to osseous posterior tension band fracture (white dotted line in C).
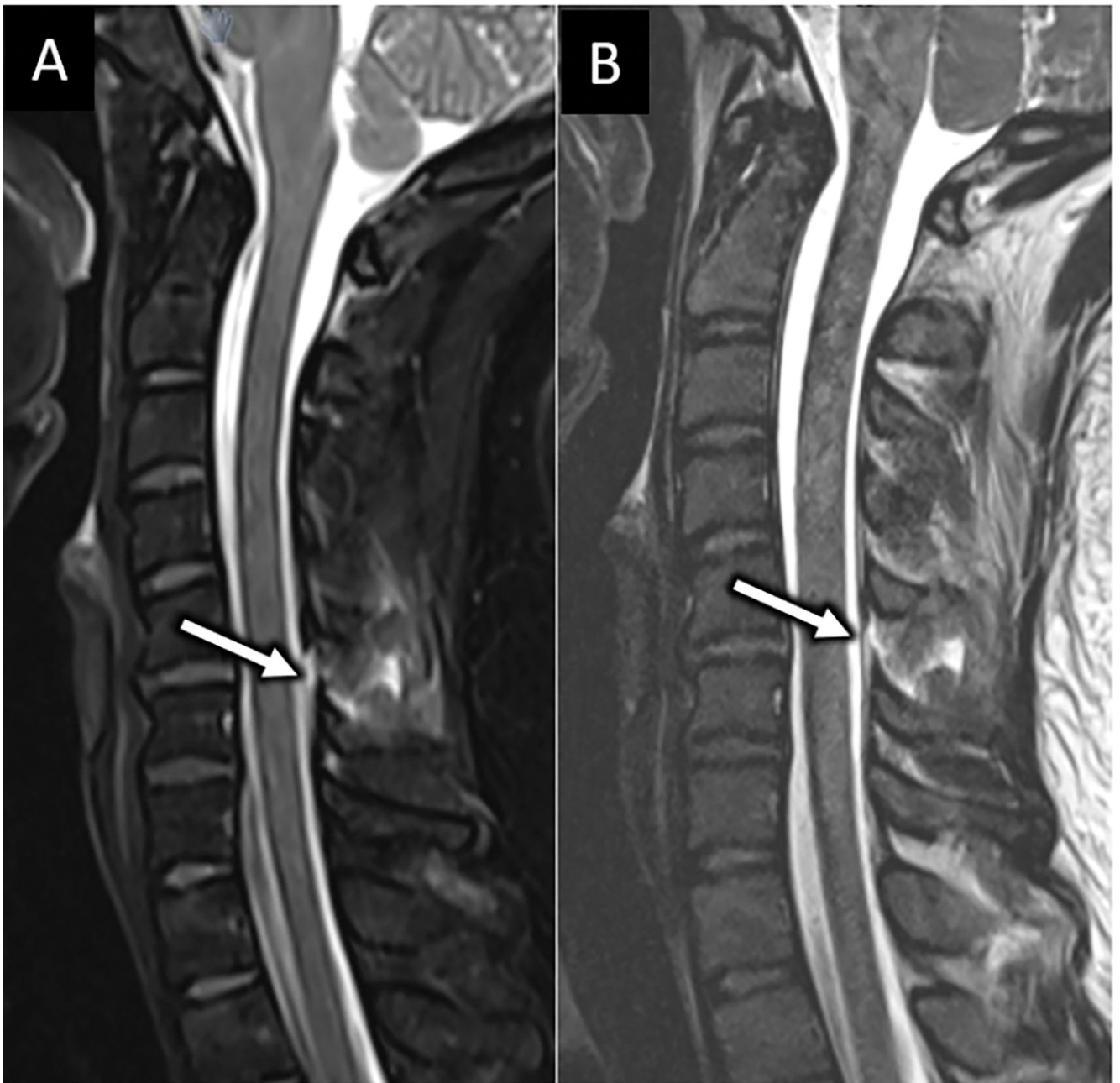
Figure 6:
MRI confirms suspected posterior ligamentous complex injury. Sagittal FS T2W (A) and
T2 SPACE (B) MR images obtained for a 33-year-old restrained passenger following motor
vehicle collision reveals abnormal edema along the posterior ligamentous complex at C5-C6
(arrow in A and B).
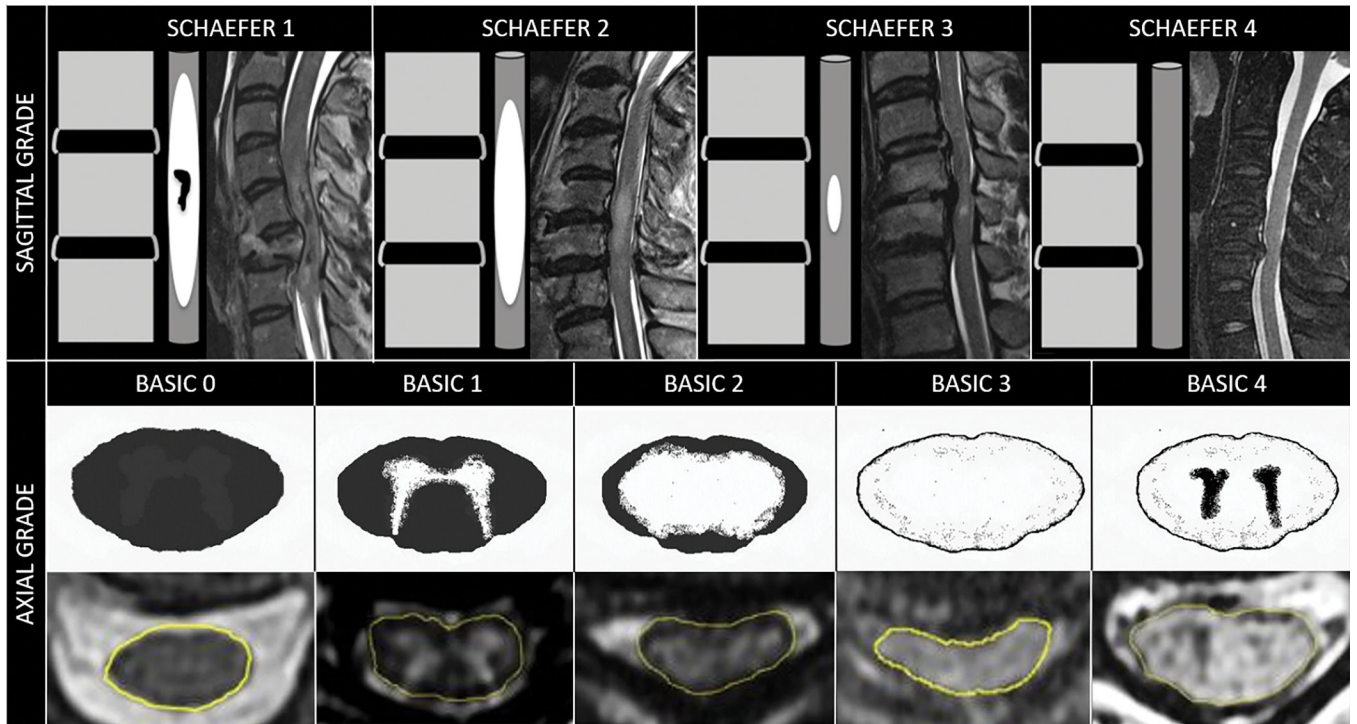
Figure 7:
Sagittal and axial MRI-based grading schema for assessment of acute traumatic spinal cord injury.
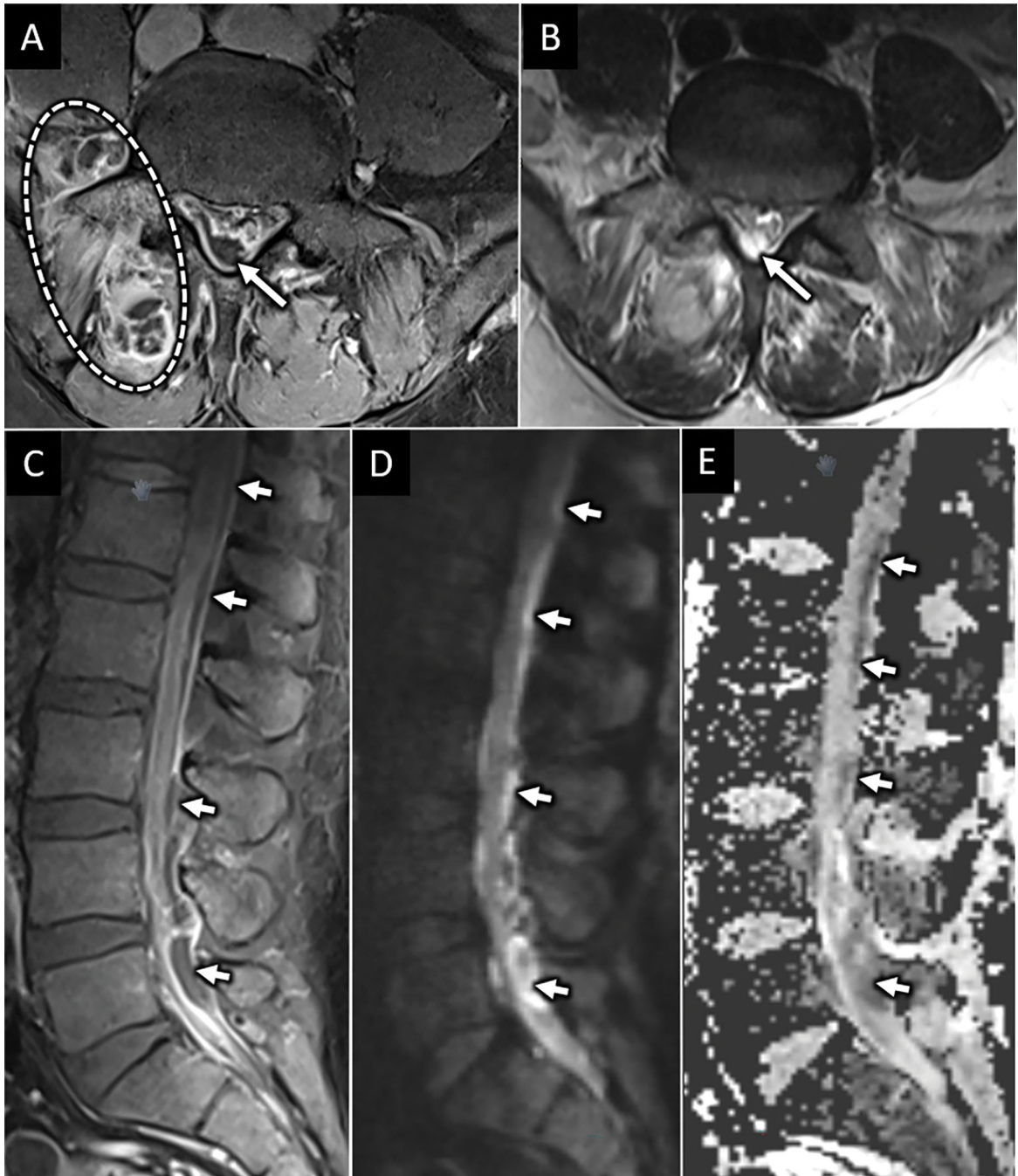
Figure 8:

Lumbar septic facet arthritis with spinal epidural abscess. Axial T1W postcontrast (A) and T2W (B) MR images from a 54-year-old male with diabetes mellitus type 2 reveals right L5-S1 peri-facet joint soft tissue enhancement and multiloculated abscess (dotted circle) consistent with septic facet arthritis. There is associated peripherally enhancing and T2 hyperintense fluid collection in the dorsal epidural space of the lower lumbar spine (arrow in A and B). Sagittal T1W postcontrast MR image shows longitudinal extension of this collection to upper lumbar levels (arrows in C). Sagittal diffusion weighted (D) and apparent

diffusion coefficient (E) images confirm abnormal reduced diffusion corresponding to the fluid collection consistent with purulent abscess (arrows in D and E).
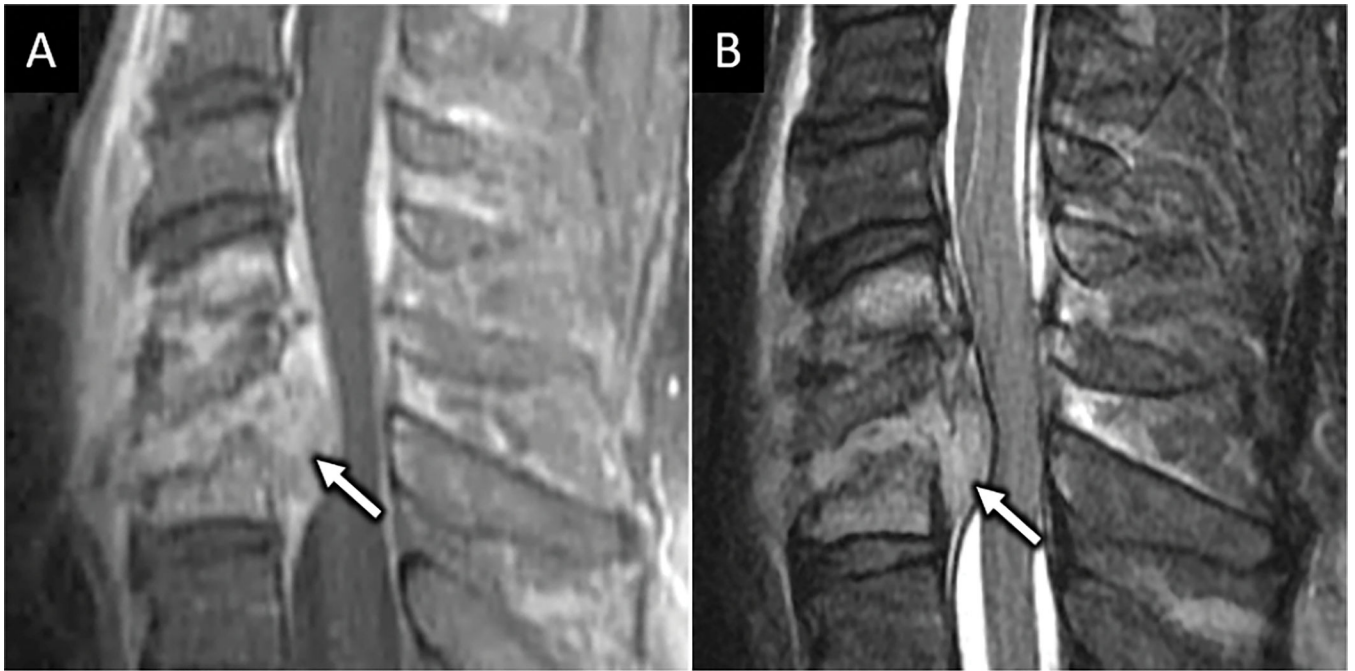
Figure 9:
DOM with epidural phlegmon resulting in spinal canal narrowing and spinal cord compression. Sagittal T1W-post contrast (A) and T2W (B) MR images centered at the mid-cervical spine show characteristic features of C4–5 and C5–6 DOM with prominent, solidly enhancing ventral epidural phlegmon (arrow in A and B).
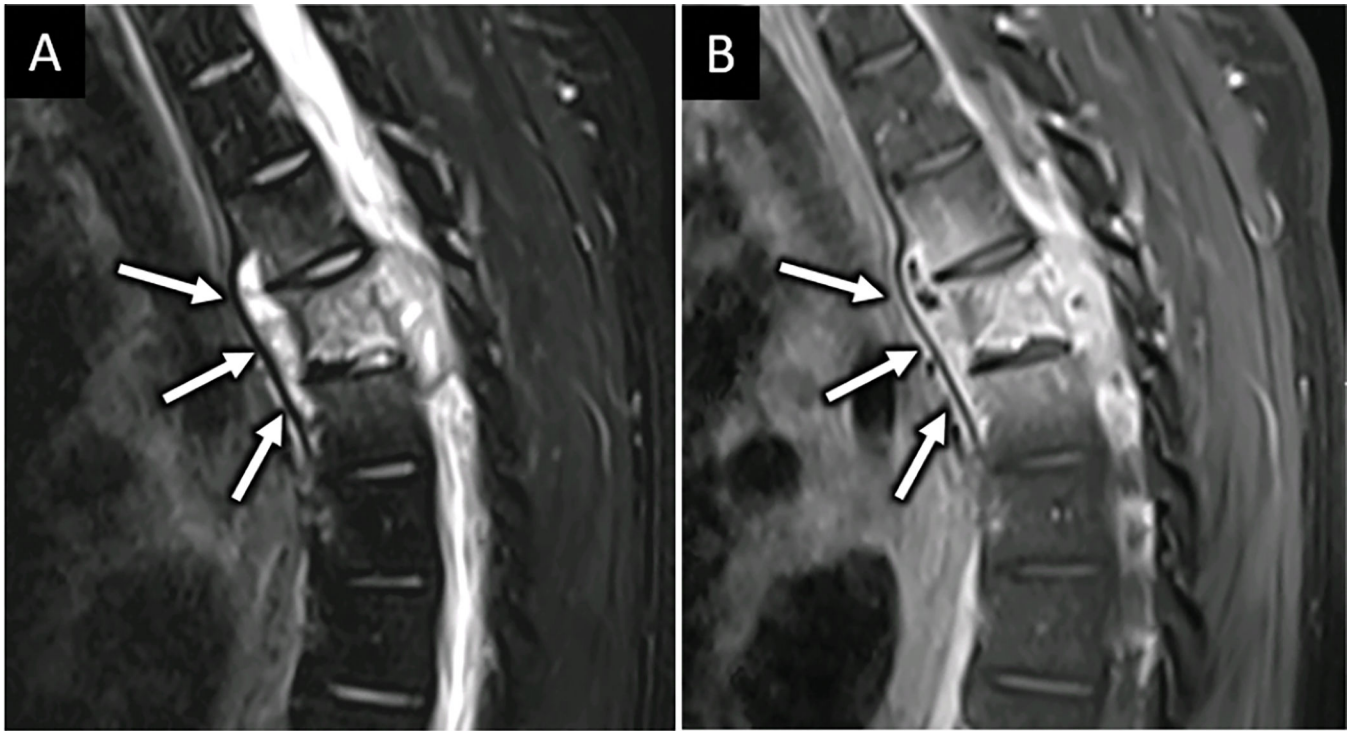
Figure 10:
Tuberculous spondylitis. Sagittal T2W FS (A) and T1W-post contrast MR images from a 31-year-old male with insidious cough, fever and weight loss reveals abnormal edema and enhancement centered at the T5 spina level notable for anterior subligamentous phlegmon extension (arrows in A and B) and relative preservation of adjacent intervertebral discs. Subsequent percutaneous biopsy confirmed mycobacterial infection.
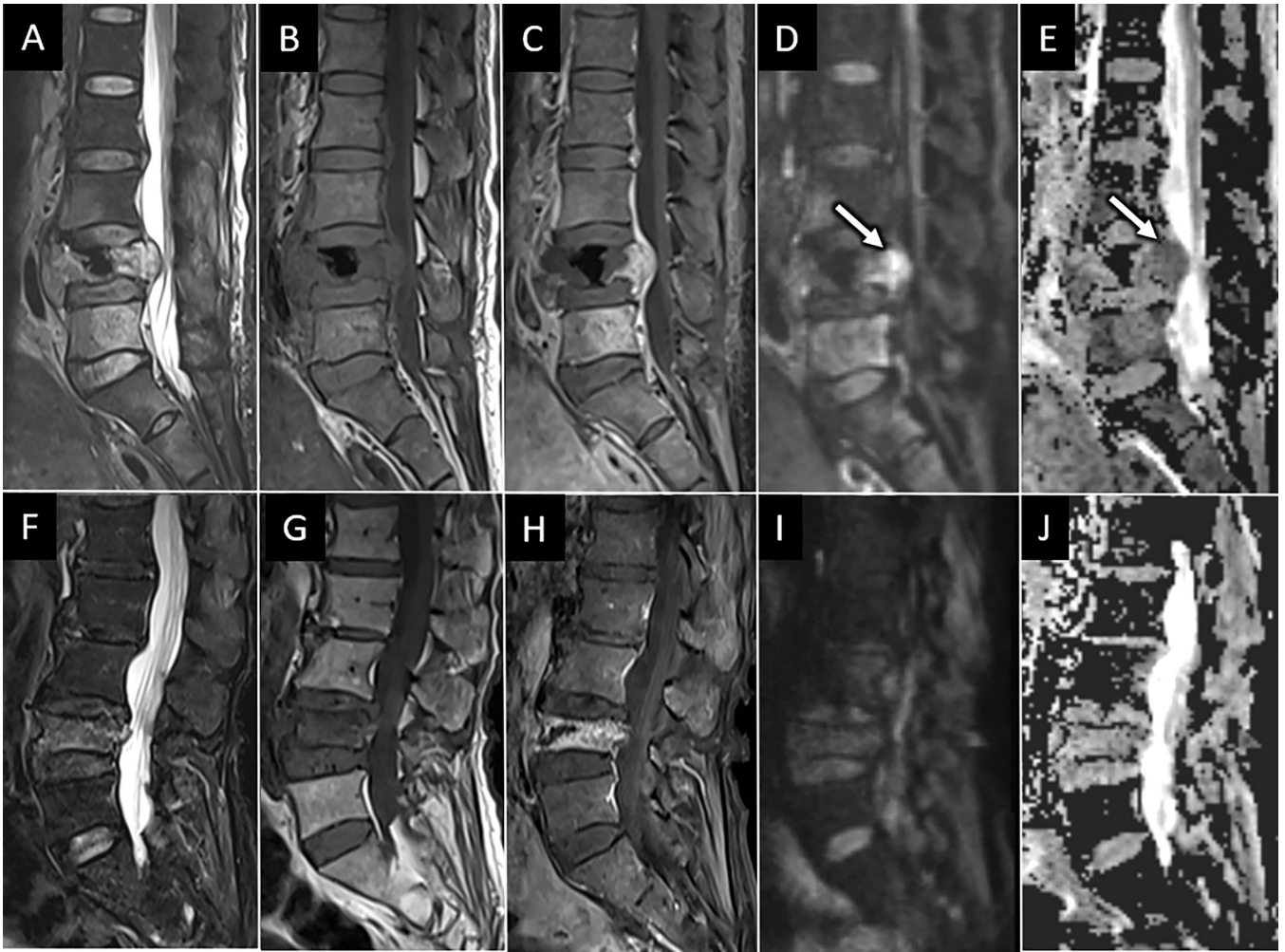
Figure 11:

Pathologic versus osteoporotic compression fractures. Sagittal T2W (A), T1W (B), T1W-post contrast (C), DWI (D), and ADC map (E) of the lumbar spine from a 59-year-old female with low back pain and breast cancer show L4 compression deformity with masslike dorsal bowing of the posterior vertebral wall encroaching on the spinal canal. Mass-like extra-osseous enhancement extending from the posterior L4 vertebral body has abnormal reduced diffusion (arrow in D and E) consistent with hypercellular tumor. Similar series of MR images (F-J) in a separate 82-year-old osteoporotic female shows L4 vertebral compression fracture with non-masslike enhancement, posterior bony retropulsion, and facilitated rather than reduced diffusion within the L4 vertebral body, consistent with osteoporotic fracture.
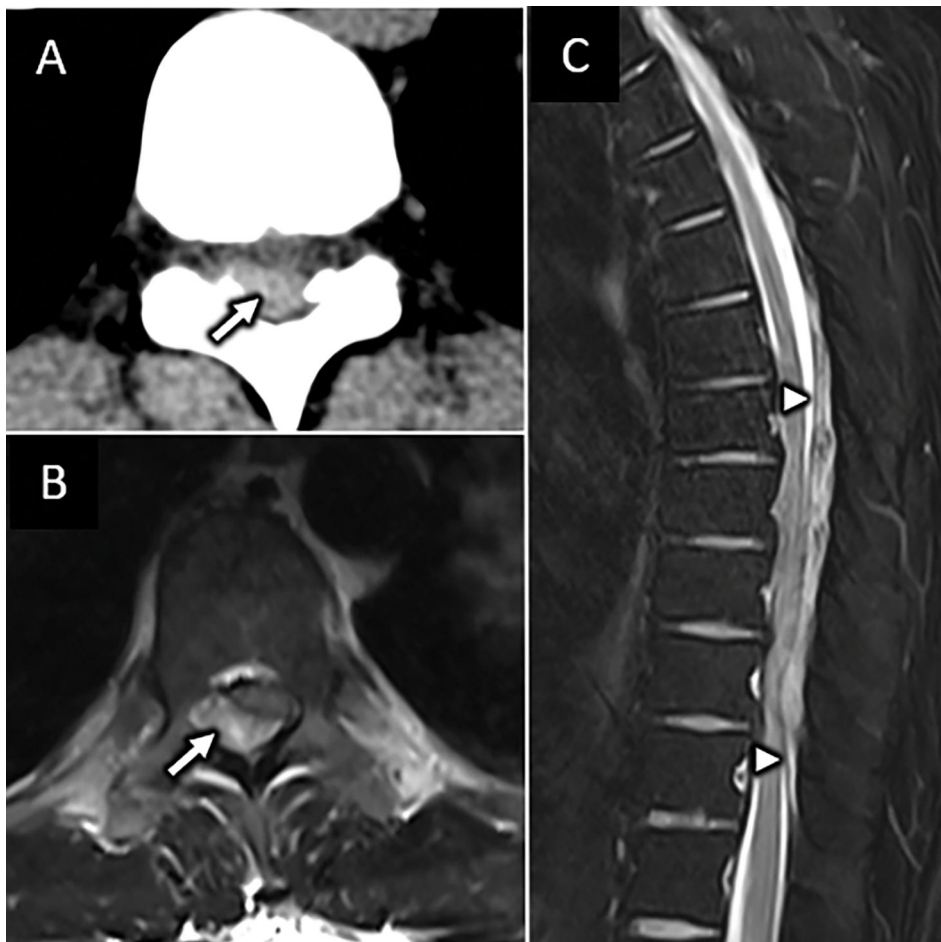
FIGURE 12:
MRI features of spontaneous epidural hematoma. Axial CT (A) and T2W MR (B)
images at the mid-thoracic level from a 41-year-old man presenting with acute onset loss
of sensory and motor function to his bilateral lower extremities immediately following
bowel movement reveal intrinsic hyperdense and T2 heterogenous expansion of the
right dorsolateral epidural space with resultant severe spinal canal stenosis and spinal
cord compression (arrow in A and B). C) Sagittal T2W image from the same patient
clearly depicts the dorsal epidural location of this collection with uplifting of the dural
membrane (arrowheads in C). Internal T2 hypointensity within the hematoma corresponds to
paramagnetic T2 shortening from blood products.

Figure 13:

Spondylotic myelopathy. A) Sag T2W FS MR image from a 46-year-old man with lower extremity weakness and fall shows severe degenerative spinal canal stenosis at the C4-C5 level with abnormal intramedullary spinal cord T2 hyperintensity centered at this level. Sagittal (B) and axial (C) T1W-post contrast images reveal transverse pattern of "pancake" like enhancement (arrow in B) which primarily involves peripheral white matter columns, consistent with spondylotic myelopathy.
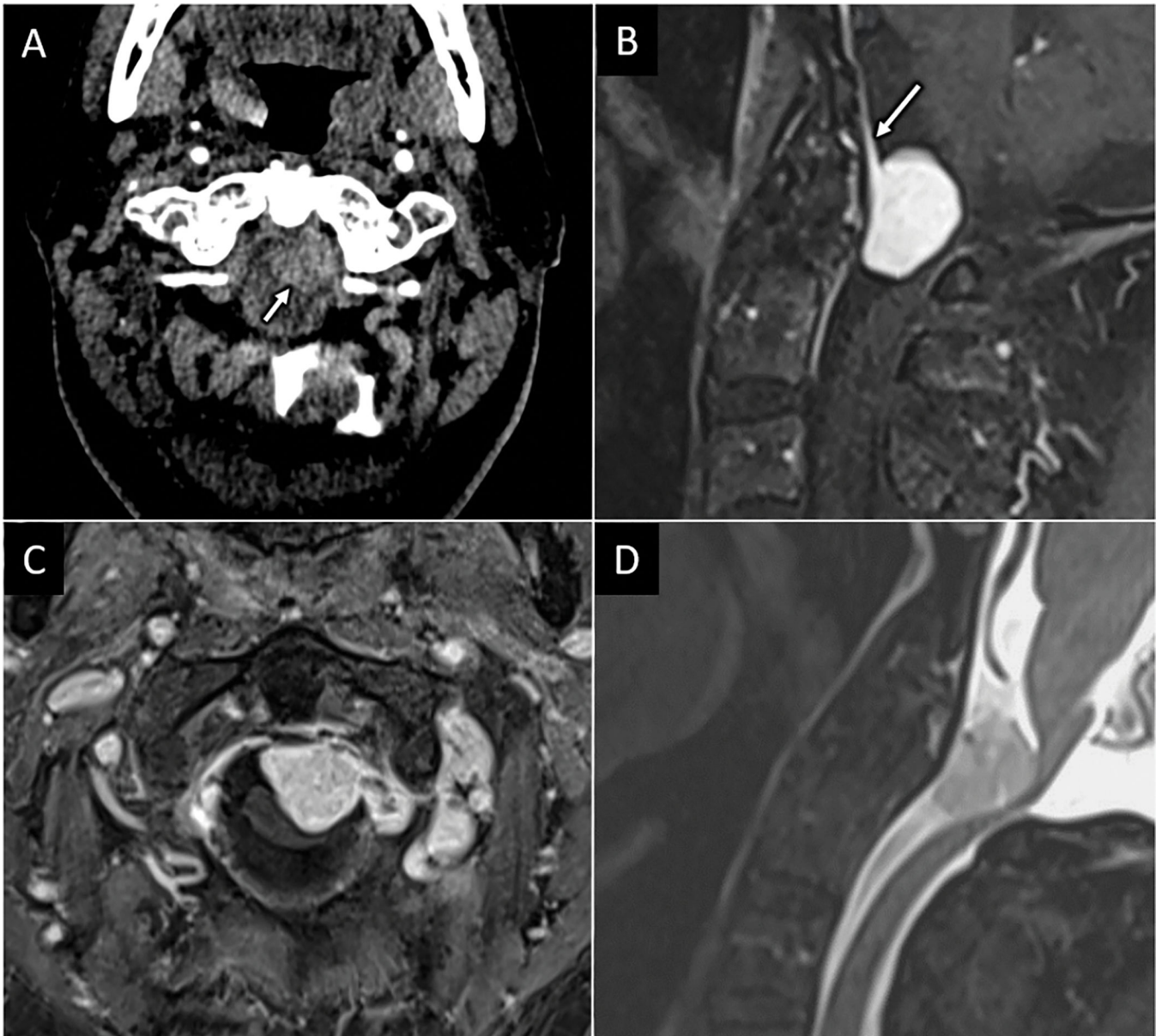
Figure 14:

Intradural compressive meningioma. Axial CT angiogram (A) performed for a 78-year-old male presenting with upper extremity paresthesia and weakness after fall shows subtle enhancing mass within the spinal canal at the C1 level (arrow in A). Sagittal (B) and axial (C) T1W FS-post contrast MR images show an intradural solidly enhancing mass with broad dural attachment and dural tail (arrow in B). Sagittal T2W FS MR image (D) shows severe spinal canal stenosis at C1 with cervicomedullary junction compression.
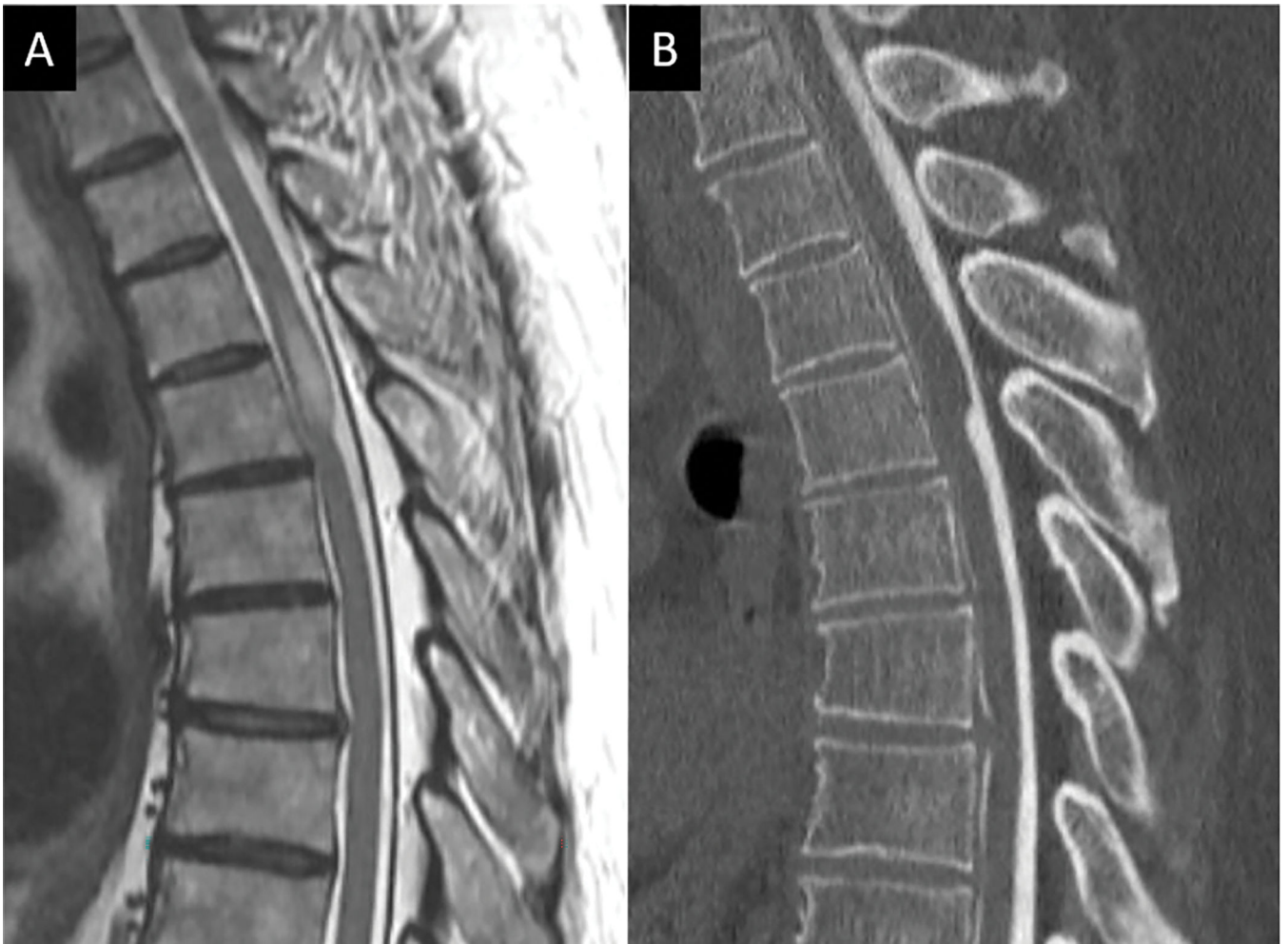
Figure 15:
Arachnoid web with compressive myelopathy. 54-year-old man presents with severe upper thoracic pain. A) Sagittal T2W MR image centered at the upper thoracic spine reveals concave indentation along the dorsal spinal cord resembling the profile of a surgical scalpel (i.e. "scalpel" sign) with intramedullary spinal cord T2 hyperintense edema above the level of spinal cord compression. Subsequent CT-myelogram (B) excluded spinal cord herniation and confirmed diagnosis of spinal arachnoid web.
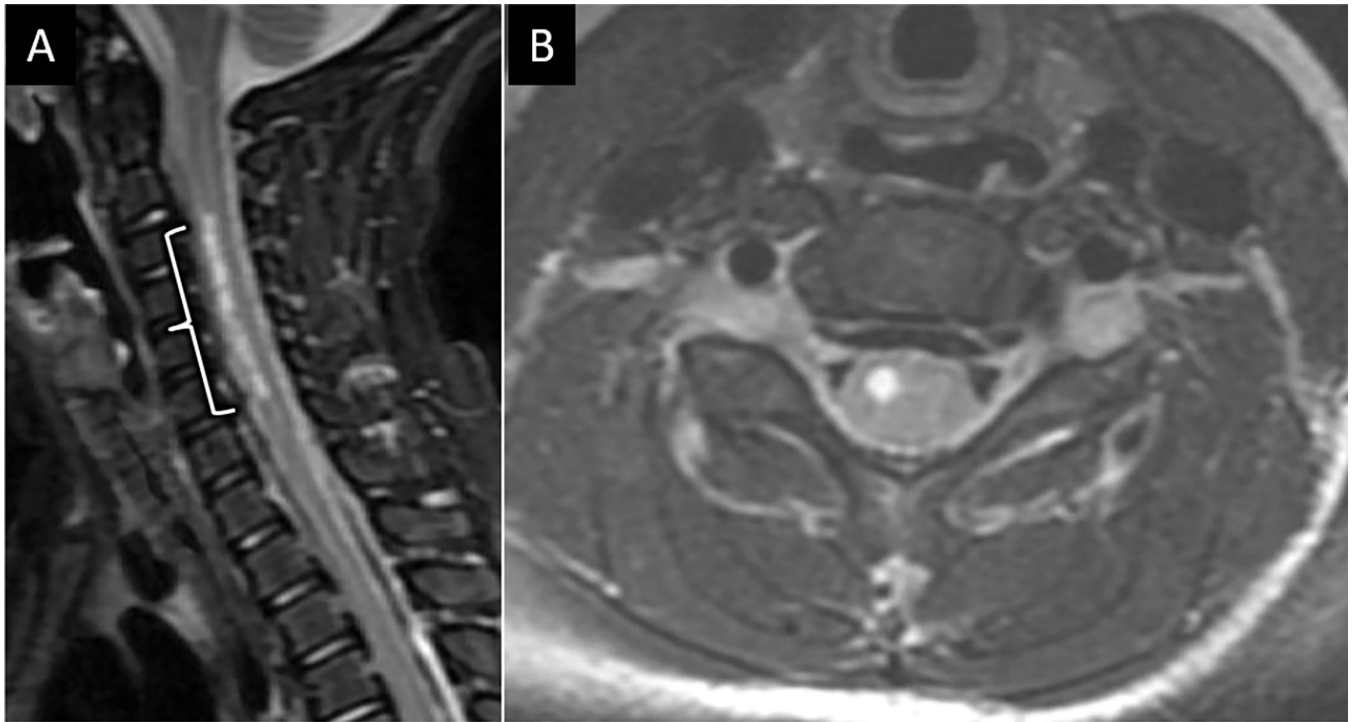
Figure 16:
Enterovirus related acute flaccid myelitis. 3-year-old boy with ten-day loss of movement in the right arm in setting of upper respiratory illness. Sagittal (A) and axial (B) T2W MR images show abnormal T2-hyperintensity spanning multiple cervical vertebral segments centered in the right frontal horn of the spinal cord.
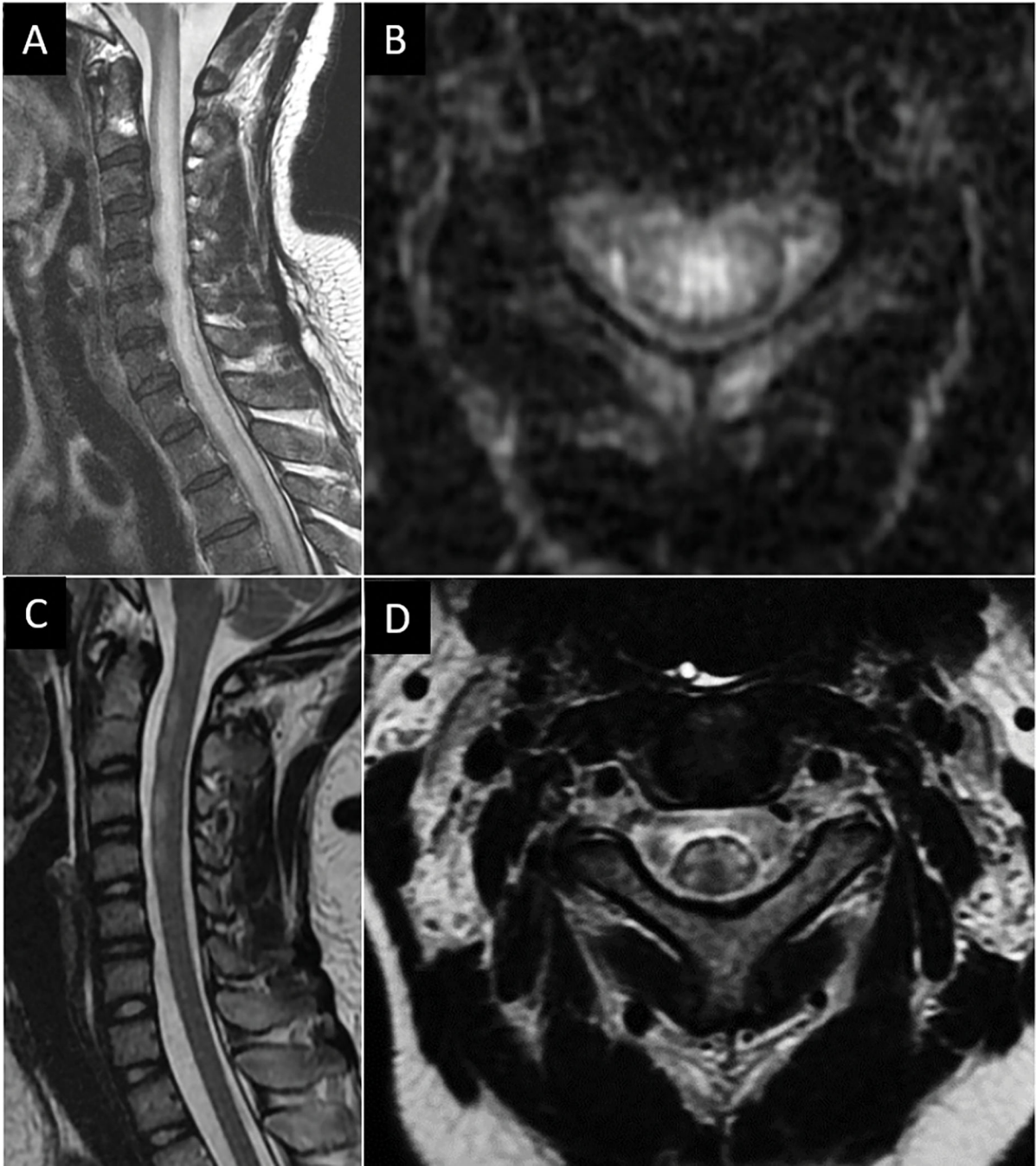
Figure 17:
Neuromyelitis optica spectrum disorder (NMOSD) and myelin oligodendrocyte glycoprotein antibody disease (MOGAD) related myelopathies. Sagittal (A) and axial (B) T2W MR images from a 51-year-old women presenting with acute onset lower extremity weakness and numbness reveals longitudinally extensive centromedullary pattern of spinal cord edema commonly seen with NMO. Sagittal (C) and axial (D) T2W MR images from a different 15-year-old patient with recurrent hospitalizations for sensory and motor deficits reveals

patchy T2 edema in the cervical spine with central gray-matter involvement resembling the letter "H" (D).
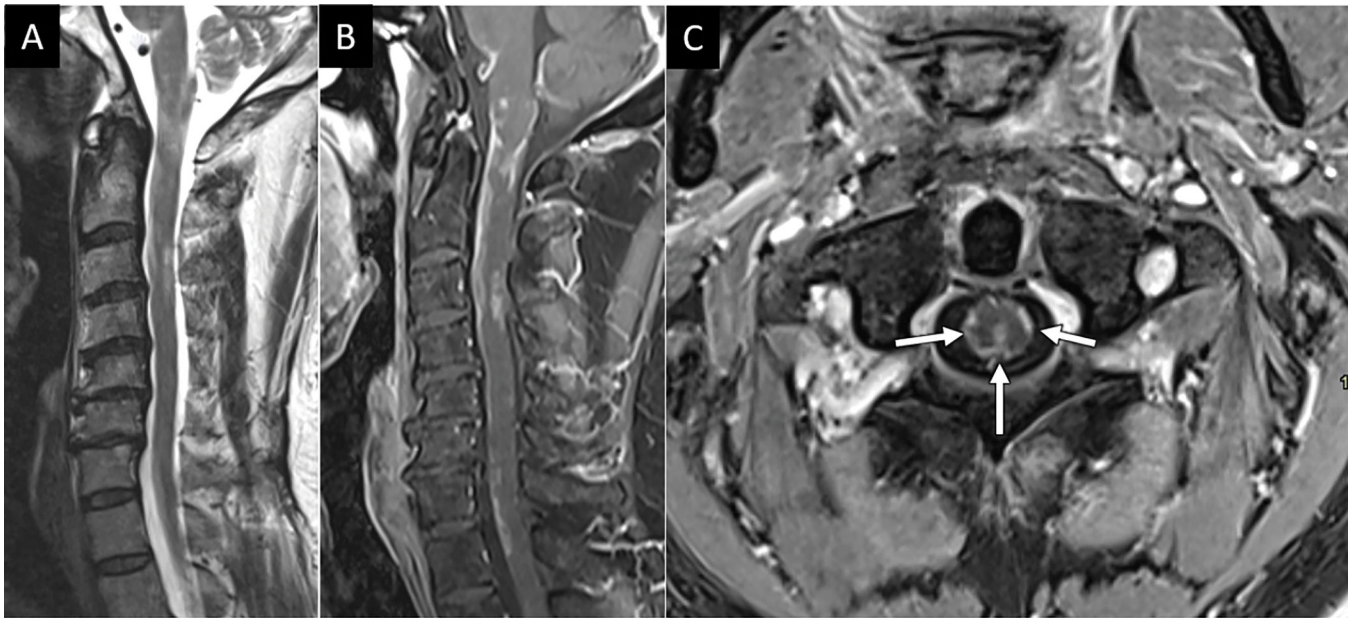
Figure 18:
Spinal neurosarcoidosis. Sagittal T2W (A) MR image of the cervical spine from a 51-year-old man with progressive numbness, spasticity, and pain reveals multifocal patchy peripheral spinal cord T2 hyperintensity. Sagittal (B) and axial (C) T1W-post contrast MR images demonstrate associated "trident" pattern of dorsal pial and infiltrative subpial spinal cord enhancement (arrows in C), a pattern typical of spinal neurosarcoidosis.
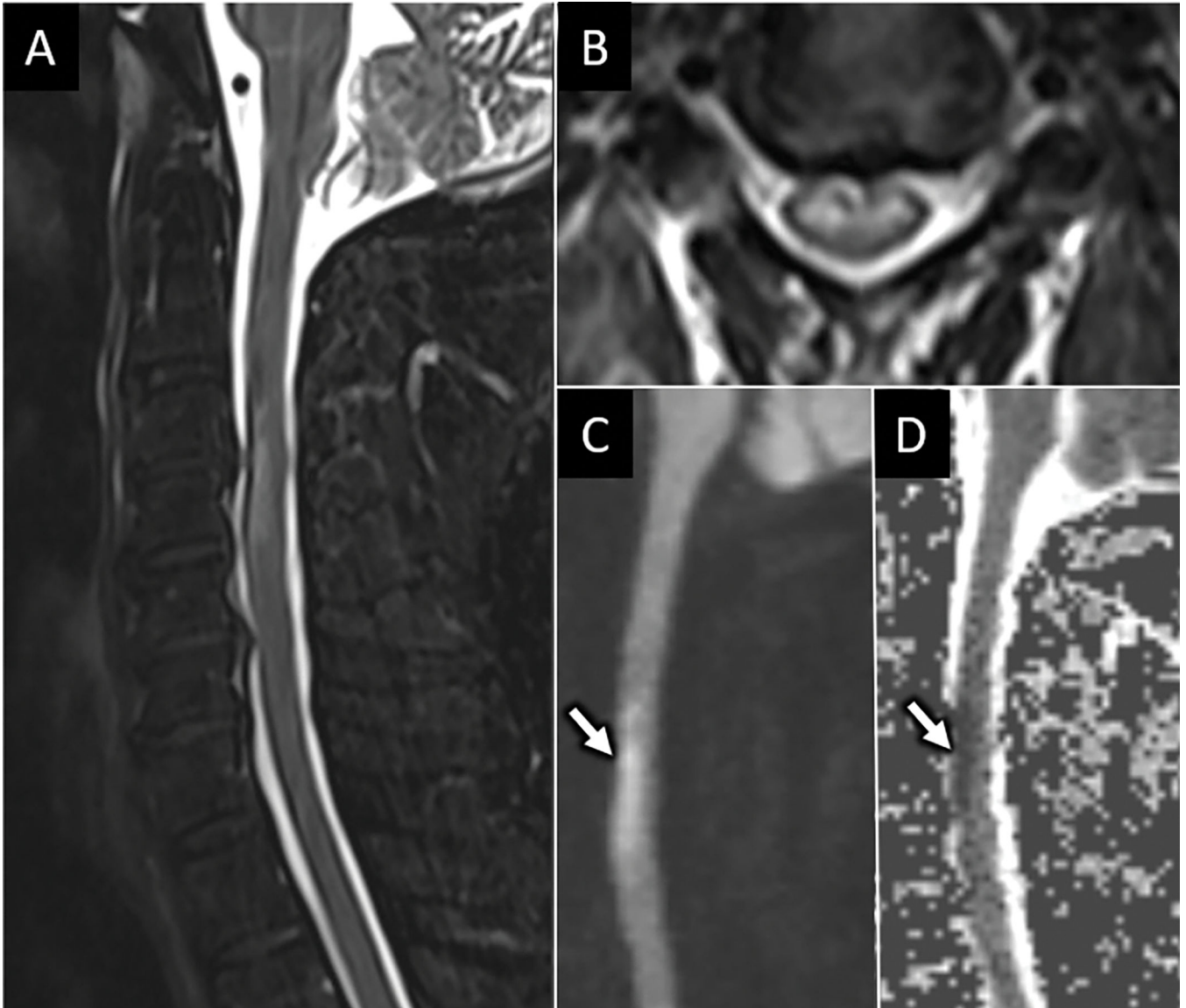
Figure 19:
Acute anterior spinal cord infarct. Sagittal (A) and axial (B) T2W FS MR images from
a 68-year-old man with acute onset upper extremity weakness following aortic aneurysm
repair shows ventral frontal-horn predominant T2 hyperintensity. Sagittal DWI (C) and
ADC map (D) from the same exam shows abnormal reduced diffusion (arrow in C and D)
corresponding with T2 signal abnormality consistent with acute anterior spinal artery infarct.
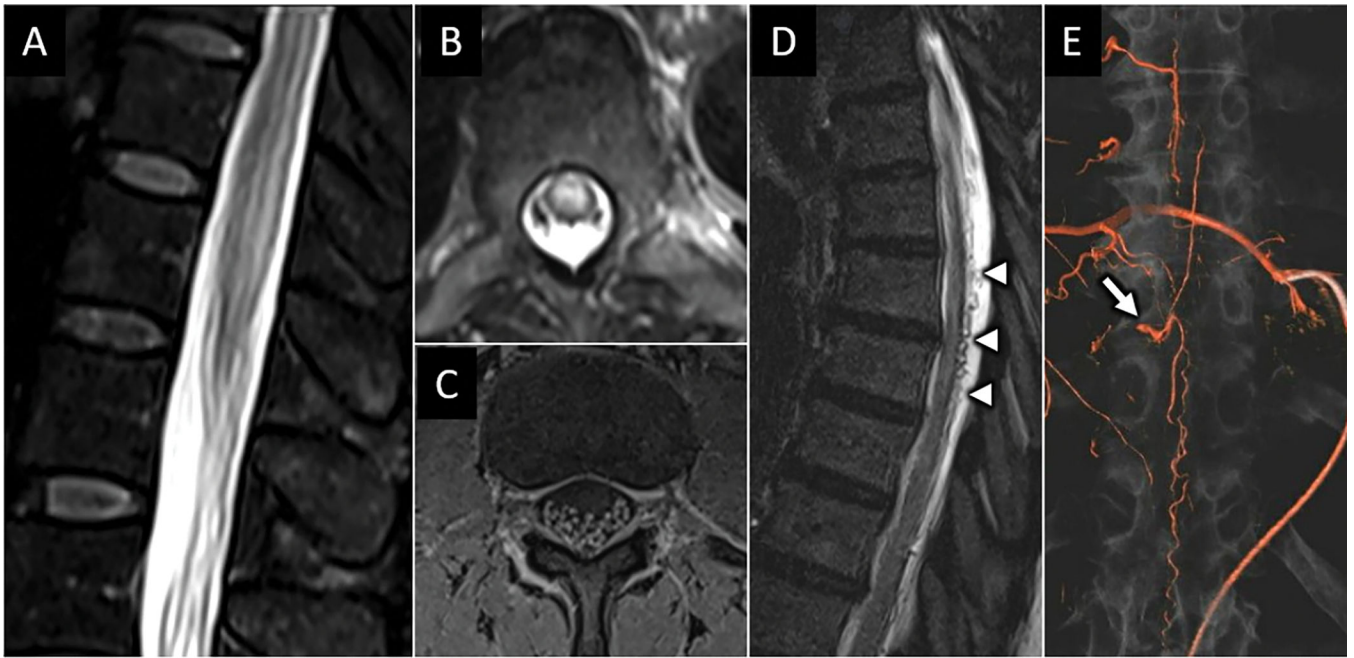
Figure 20:

Spinal dural arteriovenous fistula (sdAVF). Sagittal (A) and axial (B) T2W MR images from a 52-year-old female with rapidly progressive bilateral lower extremity weakness and urinary incontinence reveals abnormal centromedullary pattern of T2 hyperintensity in the lower spinal cord and conus. Axial T1W-post contrast image of the cauda equina (C) shows abnormal nerve root hyperenhancement. Sagittal T2W image of the thoracic spine (D) shows abnormal dilated vascular flow voids along the dorsal surface of the spinal cord (arrowheads in D). 3-dimensional reconstruction from digital subtraction angiography with selective injection of the right T9 intercostal artery reveals multiple small branches coalescing at a dilated vein within the T10-T11 neuroforamen (arrow in E) with dilated venous outflow extending cranial and caudal along the dorsum of the spinal cord, consistent with sdAVF.
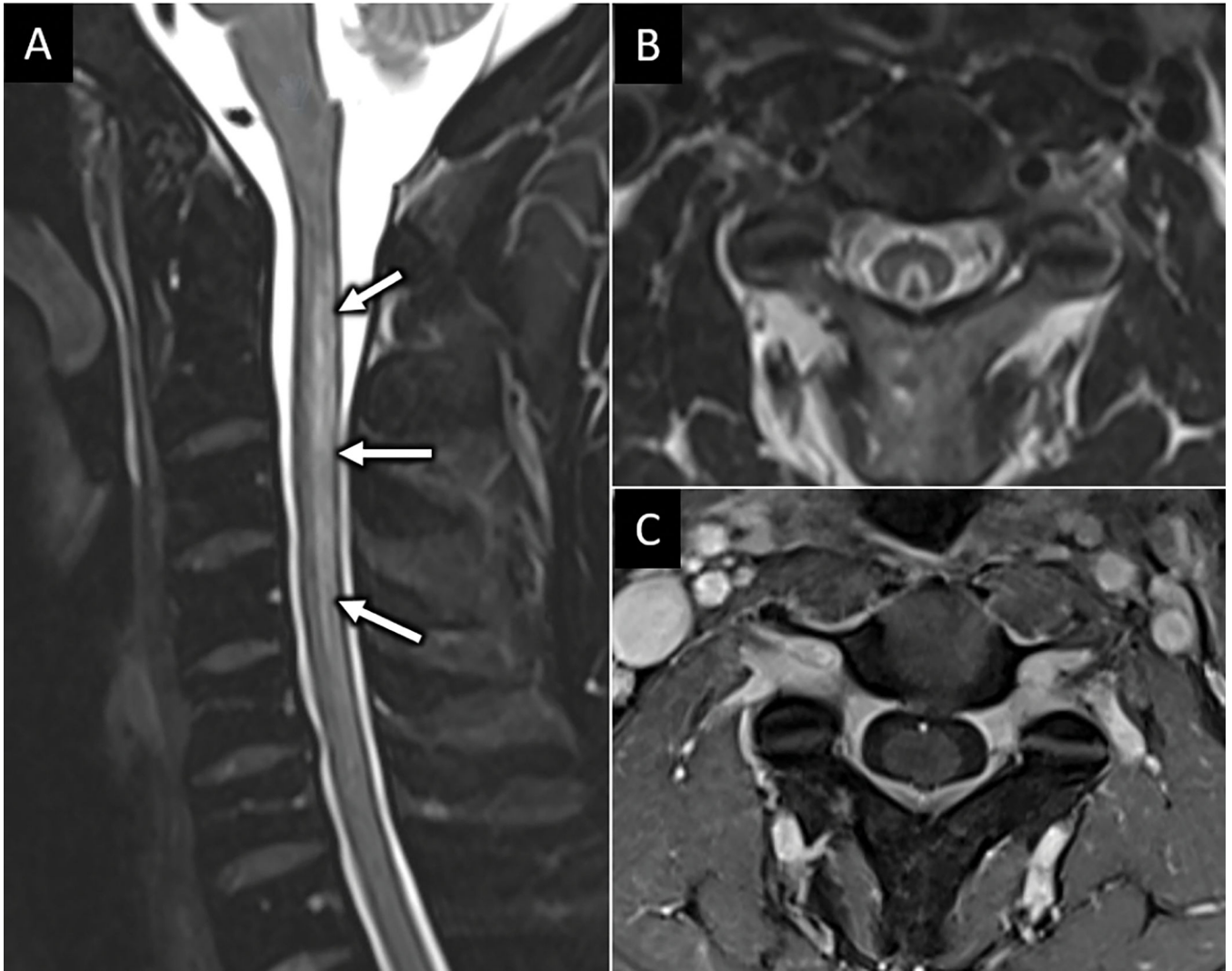
Figure 21:
Dorsal column tractopathy related to Vitamin B12 deficiency. Sagittal (A) and axial
(B) T2W MR images of the cervical spine from a 36-year-old vegetarian female with
low vitamin B12 levels and 1 week history of bilateral hand and lower extremity
numbness and gait instability demonstrates longitudinally extensive dorsal column T2
hyperintensity (arrows in A). Axial post-contrast T1W MRI (C) shows no associated
abnormal enhancement.
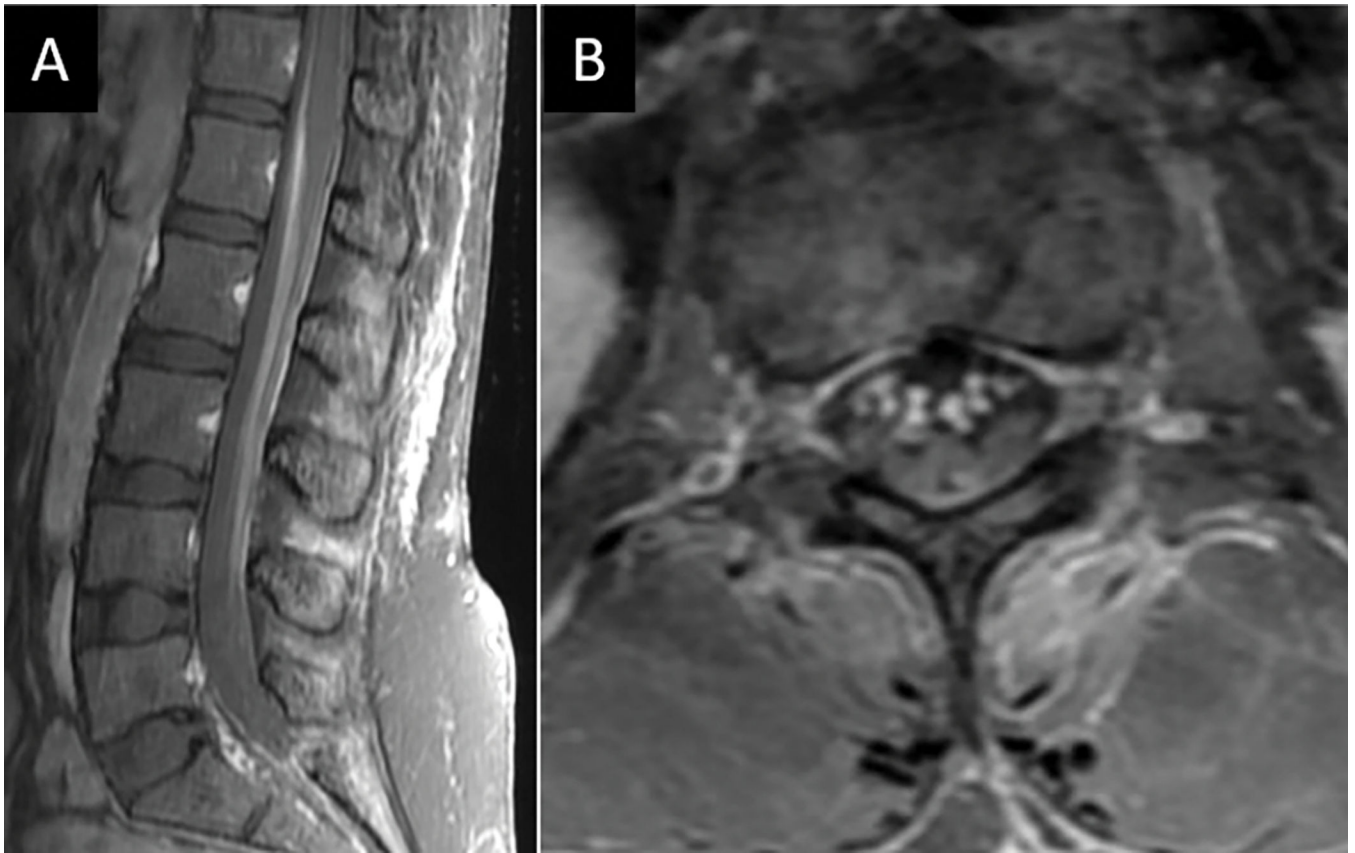
Figure 22:
Guillain Barre Syndrome. Sagittal (A) and axial (B) T1W-post contrast images of the lumbar spine show diffuse thickening and hyperenhancement of the ventral motor nerve rootlets in this 42-year-old female presenting with 1 month of rapidly progressive ascending weakness following a gastrointestinal illness.

Table 1.

AOSpine Thoracolumbar and Subaxial Cervical Spine injury Morphologic Classification[12, 13]

Type A: Compression Injuries • A0: Minor nonstructural fractures (e.g. spinous process, transverse process). • A1: Wedge compression: Single endplate fracture without posterior wall involvement • A2: Split pincer fracture: vertical fracture in coronal plane through superior and inferior endplates. • A3: Incomplete burst: Communited fracture of 1 endplate and posterior vertebral wall • A4: Complete burst: comminuted fracture of both endplates and posterior vertebral wall
Type B: Distraction Injuries • B1: Trans-osseous posterior tension band (e.g. Chance fracture) • B2: Ligamentous posterior tension band disruption • B3: Hyperextension anterior tension band disruption
Type C: Translation Injuries • Combined anterior and posterior tension band disruption with spinal displacement/dislocation
Type F: Facet injuries (subaxial cervical spine) • F1: Nondisplaced facet fracture • F2: Facet fracture with potential <1cm in height, <40% lateral mass • F3: Floating lateral mass • F4: Traumatic perched or jumped facet joints
Modifiers • M1: Possible/indeterminate posterior capsuloligamentous complex injury • M2: Critical disc herniation in presence of facet dislocation (cervical), Bone disease/abnormality (thoracolumbar) • M3: Bone disease/abnormality (cervical) • M4: vascular injury/abnormality (cervical)

Table 2.

Common Non-traumatic Compressive Pathologies

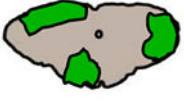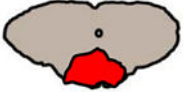| **EXTRAMEDULLARY AND EXTRADURAL** |
| --- |
| Spine infection
• Epidural abscess and/or phlegmon
• Bony retropulsion/kyphotic deformity |
| Neoplasm
• Metastases- most common include breast, prostate, lung, renal-cell carcnoma
• Primary spinal tumors including multiple myeloma and sarcoma |
| Other
• Degenerative spondylosis/Ossification posterior longitudinal ligament
• Acute disc herniation
• Spontaneous epidural hematoma |
| **EXTRAMEDULLARY AND INTRADURAL** |
| Developmental cystic lesions
• Dermoid
• Epidermoid
• Arachnoid
• Neuroenteric |
| Primary tumors
• Meningioma
• Schwannoma
• Neurofibroma
• Lipoma |
| Leptomeningeal Metastases
• Widely metastatic cancer – most common primaries include breast, lung, melanoma, colon, stomach, leukemia, lymphoma
• Aggressive primary CNS tumors – most common tumors include medulloblastoma, glioblastoma, ependymoma, germinoma, pineoblastoma, chroid plexus carcinoma |
| Other
• Arachnoid web
• Arachnoid cyst |
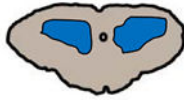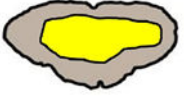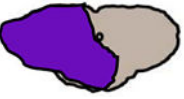
Table 3.

Transverse Patterns of Myelopathy on MRI

	Central grey matter • Infarct – anterior spinal artery occlusion • Infection – enterovirus 71, poliovirus, coxsackie A9 and A23, coxsackie B, West Nile virus, Japanese encephalitis virus • Compressive myelopathy – traumatic or atraumatic
	Peripheral white matter predominant • Demyelinating – multiple sclerosis • Infection – HIV, HSV, HTLV-1 • Neurodegenerative – ALS • Neurosarcoidosis
	Dorsal column • Subacute combined degeneration • Nitrous oxide abuse • Neurosarcoidosis • Tertiary neurosyphilis (tabes dorsalis), HIV
	Centromedullary • Infectious/parainfectious/Acute disseminated encephalomyelitis • Autoimmune – NMOSD, MOGAD • Vascular – dural AV fistula • Radiation • Idiopathic
	Irregular • Tumor • Infection – abscess • Trauma • Vascular-cavernous malformation, intramedullary AVM